Reviewed Preprint
v1 • March 18, 2026
Not revised

Reviewed Preprint
v2 • June 18, 2026
Revised by authors

The targeted cytosolic degradation of class I histone deacetylases is essential for efficient alphaherpesvirus replication

Sheng-Li Ming[1,2,3,#], Meng-Hua Du[1,2,3,#], Jia-Ming Yang[6,#], Ya-Di Guo[1,2,3], Jia-Jia Pan[1,2,3], Wei-Fei Lu[1,2,3], Jiang Wang[1,2,3,5], Lei Zeng[1,2,3] ✉, Bei-Bei Chu[1,2,3,4,5] ✉

[1]College of Veterinary Medicine, Henan Agricultural University, Zhengzhou, China • [2]Key Laboratory of Animal Biochemistry and Nutrition, Ministry of Agriculture and Rural Affairs, Beijing, China • [3]Key Laboratory of Animal Growth and Development of Henan Province, Henan Agricultural University, Zhengzhou, China • [4]International Joint Research Center of National Animal Immunology, Henan Agricultural University, Zhengzhou, China • [5]Ministry of Education Key Laboratory for Animal Pathogens and Biosafety, Zhengzhou, China • [6]State Key Laboratory of Membrane Biology, School of Pharmaceutical Sciences, Tsinghua University, Beijing, China

For correspondence:
zenglei@henau.edu.cn
chubeibei@henau.edu.cn

[#] These authors contributed equally

Competing interests: No competing interests declared

Funding: See page 16

Reviewing editor: John W Schoggins, The University of Texas Southwestern Medical Center, United States

eLife Assessment

This **valuable** study demonstrates that alpha herpes viruses trigger nuclear export of HDACs, which are then degraded in an MDM2-dependent manner. This virus-driven process leads to histone hyperacetylation and activation of the DNA damage response, which promotes viral replication. The presented evidence is mostly **solid**, but the mechanistic conclusions could be further strengthened with additional controls.

https://doi.org/10.7554/eLife.110309.2.sa3

Abstract

Viral infection triggers a robust DNA damage response (DDR), reshaping the host chromatin landscape to facilitate viral replication. Here, we uncover a novel mechanism by which alphaherpesviruses exploit the DDR pathway. We demonstrated that herpes simplex virus 1 (HSV-1) and pseudorabies virus (PRV) induced selective degradation of class I histone deacetylases (HDAC1/2), leading to histone hyperacetylation and subsequent DDR activation. Strikingly, viral infection promoted nuclear export of HDAC1/2, followed by MDM2-mediated K63-linked polyubiquitination and proteasomal degradation in the cytoplasm. Pharmacological inhibition of either DDR signaling or HDAC1/2 nuclear export significantly affected viral replication *in vitro* and *in vivo*. Our findings reveal a unique viral strategy to hijack host epigenetic regulation for efficient replication and identify potential therapeutic targets for alphaherpesvirus infections.

Introduction

HSV-1 is a widespread neurotropic virus that infects more than two-thirds of the global population under the age of 50[1]. After initial infection of mucosal epithelia and neuronal tissues, HSV-1 establishes lifelong latency within sensory ganglia[2]. Clinically, HSV-1 infection can present as oral or genital lesions and, in severe instances, may progress to herpes simplex encephalitis—a potentially fatal inflammation of the brain[3, 4]. Emerging evidence suggests a plausible association between HSV-1 and neurodegenerative conditions such as Alzheimer's disease, linking chronic neuroinflammation and neuronal impairment to persistent viral infection[5, 6]. To sustain lifelong infection, HSV-1 employs sophisticated strategies to evade host immune defenses and maintain latent reservoirs.

Epigenetic regulation plays a critical role in governing HSV-1 latency and reactivation[7, 8]. During latency, the virus coopts host histone deacetylases (HDACs) to enforce viral genomic silencing through chromatin condensation[9]. Although HDAC1 and HDAC2 are central to chromatin stability and DNA damage response (DDR), their roles during alphaherpesvirus infection appear complex and context-dependent[10]. While these enzymes contribute to viral repression during latency[11], their potential involvement in promoting lytic replication—whether through degradation or functional inactivation—has remained inadequately explored.

Histone acetylation, a pivotal epigenetic modification that modulates chromatin accessibility and transcriptional activity, is dynamically regulated by histone acetyltransferases (HATs), which add acetyl groups to activate gene expression, and HDACs, which remove these groups to enforce repression[12, 13]. The HDAC family is categorized into four classes: Class I (HDAC1, 2, 3, 8), Class IIa/b, Class III (sirtuins), and Class IV (HDAC11)[14]. Among these, Class I HDACs—particularly HDAC1 and HDAC2—are indispensable for chromatin remodeling, genomic integrity, and immune modulation[15–18]. These enzymes contribute to host antiviral defense by fine-tuning the expression of immune-related genes. Nevertheless, the mechanisms through which HSV-1 overcomes this transcriptional repression remain incompletely understood[18].

HDAC1 serves as a key regulator of chromatin dynamics and innate immune signaling, interfacing with critical pathways such as NF-κB, JAK-STAT, and Toll-like receptor cascades to shape antiviral responses[19–22]. For example, in lung epithelial cells, HDAC1 facilitates STAT1 phosphorylation and enhances interferon-stimulated gene (ISG) activation, thereby restricting influenza A virus replication[23]. This underscores the dual function of HDAC1 in both epigenetic control and immune regulation. However, the specific strategies used by HSV-1 to manipulate HDAC1/2—particularly through ubiquitin-mediated degradation—to circumvent host immunity and enhance viral replication have not been clearly defined.

This study reveals that HSV-1 induces the degradation of HDAC1/2 via an MDM2-dependent ubiquitination mechanism, resulting in elevated histone acetylation, chromatin relaxation, and activation of DNA damage response pathways that collectively enhance viral replication. These findings offer novel insights into the epigenetic subversion strategies employed by HSV-1 and underscore the therapeutic potential of targeting the HDAC–MDM2 axis in the treatment of herpesvirus infections.

Materials and Methods

Mice

Female C57BL/6J mice (6–8 weeks old) were purchased from the Experimental Animal Center of Zhengzhou University (Zhengzhou, China) and housed in specific-pathogen-free facilities under controlled environmental conditions, including a 12-hour light-dark cycle and a temperature of 22°C. For in vivo infection studies, mice were anesthetized with isoflurane prior to intranasal inoculation with HSV-1, at a dose of 1×10^6 PFU per mouse in a total volume of 30 μL PBS. Clinical signs—including ruffled fur, hunched posture, reduced mobility, and body weight loss 15%—were monitored daily. On day 15 post-infection, mice were humanely euthanized by intravenous injection of sodium pentobarbital (90 mg/kg), following the “Guidelines for the Euthanasia of Laboratory Animals”. Immediately thereafter, tissues—including liver, spleen, lung, brain, and draining cervical lymph nodes—and serum were harvested under sterile conditions. All tissues were snap-frozen in liquid nitrogen within 60 seconds of excision and stored at −80°C until further analysis. Samples were processed for Western blotting. All procedures were in accordance.

Reagents and plasmids

Reagents were sourced as follows: Leptomycin B (HY-16909), MG-132 (HY-13259), 3-MA (HY-19312), cycloheximide (HY-12320), and chloroquine (HY-17589A) were purchased from MedChemExpress; berzosertib (S7102) was purchased from Selleck; DMSO (W387520) was purchased from Sigma-Aldrich. Unless otherwise specified, all inhibitors were added at 1 hour post-infection (hpi), after completion of viral adsorption and entry, to avoid interference with early viral processes.

Antibodies against CHK1 (25887-1-AP), CHK2 (13954-1-AP), RAD51 (14961-1-AP), β-actin (66009-1-lg), P53 (10442-1-AP), HDAC1 (10197-1-AP), HDAC2 (12922-3-AP), HDAC4 (17449-1-AP), HDAC6 (12834-1-AP), HDAC11 (67949-1-Ig), and EGFP (50430-2-AP) were purchased from Proteintech; antibodies against p-P53 (9286), p-ATM (13050), ATM (2873), ATR (13934), p-ATR (2853), p-CHK1 (12302), p-CHK2 (2197), γ-H2AX (80312), H3 (4499), H4K8ac (2594), H4K12ac (13944), H4 (13919), H2AX (7631), H3K9ac (4658), H3K27ac (8173), UB (20326), and MDM2 (86934) were purchased from Cell Signaling Technology; H3K56ac antibody (07-677) was purchased from Millipore; ICP4 antibody (ab6514) was purchased from Abcam; ICP0 antibody (sc-53070) was purchased from Santa Cruz Biotechnology; FLAG antibody (F7425) was purchased from Sigma-Aldrich; HA antibody (A00169) was purchased from GenScript.

HDAC1 and HDAC2 coding sequences were amplified from HEK293 cell cDNA and cloned into p3×FLAG-CMV-10 to generate FLAG-tagged expression constructs. MDM2 coding sequence was amplified and inserted into pEGFP-C1 to produce EGFP-MDM2. Site-directed mutagenesis was performed using the QuikChange Site-Directed Mutagenesis Kit (Agilent Technologies, 200523) per the manufacturer's instructions to generate: FLAG-HDAC1 K8R, FLAG-HDAC1 K10R, FLAG-HDAC1 K31R, FLAG-HDAC1 K50R, FLAG-HDAC1 K58R, FLAG-HDAC1 K66R, FLAG-HDAC1 K74R, FLAG-HDAC1 K89R, FLAG-HDAC2 K75R, FLAG-HDAC1 (aa 1–329), FLAG-HDAC1 (aa 329–482), FLAG-HDAC1 (aa 1–100), FLAG-HDAC1 (aa 100–329),, and EGFP-MDM2ΔRING (aa 1–435). FLAG-HDAC1 ΔNES (residues 207–216 deleted), in which the deletion encompasses the CRM1-dependent nuclear export signal as predicted by NESmapper. HA-tagged ubiquitin constructs [HA-UB (WT), HA-UB (K48), HA-UB (K63)] were provided by Dr. Bo Zhong (College of Life Sciences, Wuhan University, China).

Cells

Cell lines (HeLa/ATCC CL-82, Vero/ATCC CL-81, 3D4/21/ATCC CRL-2843, HEK293T/ATCC CRL-11268) were cultured in DMEM or RPMI 1640 supplemented with 10% fetal bovine serum (FBS), 1% penicillin/streptomycin, and 1% L-glutamine at 37°C under 5% CO_2 in a humidified incubator. For transient transfections, DNA constructs were delivered to HeLa and HEK293T cells using Lipofectamine 3000 (Invitrogen, L3000001) per the manufacturer's protocol.

To generate shRNA-mediated knockdown cell lines, HEK293T cells were co-transfected with control or gene-specific shRNA (Table S1), packaging plasmid psPAX2, and envelope plasmid pMD2.G. Post-transfection (6 h), medium was replaced, and lentiviral particles were harvested at 48 hours. Parental cells were infected with viral supernatant and selected with puromycin to establish stable knockdown lines.

To generate siRNA-mediated knockdown cell lines, HeLa cells were transfected with either a non-targeting control siRNA or gene-specific siRNAs (Table S1) using Lipofectamine™ RNAiMAX(Invitrogen, 13778030). Transfection was performed at a confluency of approximately 30%, and target gene and protein expression levels were assessed 48 hours post-transfection.

Viruses

HSV-1 strain F (provided by Dr. Chun-Fu Zheng, University of Calgary, Canada) and PRV-QXX were propagated per established protocols [24]. Viral titers were determined by plaque assays in Vero cells. For in vitro infections, cells were infected with HSV-1 or PRV-QXX at an MOI of 1. For in vivo studies, mice were intranasally inoculated with HSV-1 (1×10^6 pfu/mouse).

Immunoblotting, ubiquitination and Co-immunoprecipitation (Co-IP)

For immunoblotting, cells were lysed in RIPA buffer [50 mM Tris-HCl (pH 8.0), 150 mM NaCl, 1% Triton X-100, 1% sodium deoxycholate, 0.1% SDS, 2 mM $MgCl_2$] supplemented with protease/phosphatase inhibitors. Proteins were resolved by SDS-PAGE, transferred to PVDF membranes, and blocked with 5% nonfat milk in TBST (1 hour, RT). Membranes were incubated

with primary antibodies (overnight, 4°C), then HRP-conjugated secondary antibodies (1 hour, RT). Signals were detected using Laminate Crescendo Western HRP Substrate (Millipore, Cat. No. WBLUR0500) on a GE AI600 imager.

For ubiquitination assay, cells were lysed in IP buffer [50 mM Tris-HCl (pH 7.4), 150 mM NaCl, 1% NP-40, 1% sodium deoxycholate, 5 mM EDTA, 5 mM EGTA] and clarified (16,000 × *g*, 10 minutes, 4°C). Subsequently, 900 µl aliquots were incubated with 40 µl of a 1:1 slurry of Sepharose beads conjugated to anti-HDAC1 or anti-FLAG mouse monoclonal antibodies (4°C, 4 hours). Beads were washed four times with IP buffer, eluted in SDS sample buffer (10 minutes, boiling), and analyzed by immunoblotting.

For Co-IP assay, cells were lysed in Co-IP buffer [50 mM Tris-HCl (pH 7.4), 150 mM NaCl, 1% NP-40, 5 mM EDTA, 5 mM EGTA] and clarified (16,000 × *g*, 10 minutes, 4°C). Aliquots (900 µl) were incubated with 40 µl of a 1:1 slurry of Sepharose beads conjugated to IgG (GE Healthcare) or anti-FLAG mouse monoclonal antibody (4°C, 4 hours). Beads were washed three times with Co-IP buffer, eluted in SDS sample buffer (10 minutes, boiling), and analyzed by immunoblotting.

Immunofluorescence assay

Cells were fixed in 4% paraformaldehyde at room temperature for 20 min on coverslips in 12-well plates. Following three washes with PBS, cells were permeabilized with 0.2% Triton X-100 for 20 min and subsequently blocked with 10% FBS. Specific primary antibodies, diluted in 10% FBS, were then applied to the cells and incubated for 1 h at room temperature. After three PBS washes, cells were exposed to the appropriate secondary antibodies, also diluted in 10% FBS, for 1 h at room temperature. Nuclei were stained with DAPI for 5 min at room temperature, mounted using Prolong Diamond (Invitrogen), and visualized using a Zeiss LSM 800 confocal microscope.

Comet assay

Cells were seeded in 6-well plates and treated accordingly. Frosted microscope slides were coated with 0.5% normal melting point agarose. A mixture of 10 µL DMEM containing around 10,000 cells and 75 µL of 0.7% low melting point agarose was layered onto the pre-coated agarose. An additional 75 µL of 0.7% low melting point agarose formed a third layer. The slides were lysed in a buffer containing 10 mM Tris-HCl, pH 10.0, 2.5 M NaCl, 100 mM Na2EDTA, 1% Triton X-100, and 10% DMSO for 2 hours at 4°C. Post-lysis, the slides were treated with an electrophoresis solution (300 mM NaOH, 1 mM Na2EDTA, pH >13) for 40 minutes, electrophoresed at 20 V (~300 mA) for 25 minutes, and neutralized with 0.4 mM Tris-HCl (pH 7.5). Subsequently, cells were stained with propidium iodide (PI, 5 µg/mL) and examined using a Zeiss LSM 800 confocal microscope. DNA damage was assessed based on tail moment using CometScore software.

qRT-PCR analysis

Total RNA was isolated using TRIzol reagent (TaKaRa) and reverse-transcribed into cDNA with the PrimeScript RT reagent kit (TaKaRa). qRT-PCR was performed in triplicate using SYBR Premix Ex Taq (TaKaRa) according to the manufacturer's protocol. Expression levels were normalized to β-actin as an internal reference. Melting curve analysis confirmed amplification specificity by verifying single-product formation in all reactions. Relative gene expression was calculated using the $2^{-\Delta\Delta Ct}$ method. Primer sequences are provided in Table S1

Plaque assay

Vero cells (seeded in six-well plates) were grown to confluence, infected with serially diluted viruses (10^{-1}–10^{-7}; 1 hour, 37°C), and washed with PBS to remove residual inoculum. DMEM containing 1% methylcellulose (4 mL/well) was added, and cells were incubated for 4–5 days. Post-incubation, cells were fixed with 4% paraformaldehyde (15 minutes), stained with 1% crystal violet (30 minutes), and plaques were quantified.

Statistical analysis

Statistical analyses were performed using GraphPad Prism 8 software. Comparisons between two groups were evaluated using a two-tailed Student's *t*-test. Significance was defined as $P < 0.05$. Data are presented as mean ± SD of three independent experiments. Kaplan-Meier survival curves were generated and analyzed for mouse survival assessment.

Results

HSV-1 infection promotes HDAC1/2 degradation and histone hyperacetylation

Post-translational modifications of histones play a critical role in regulating chromatin remodeling and gene expression. HDACs, a highly conserved enzyme family [25], catalyze the removal of acetyl groups from histones, thereby promoting chromatin condensation and transcriptional repression. To investigate the effect of HSV-1 infection on HDAC expression and histone acetylation, we examined the protein levels of key HDAC isoforms following viral infection. Immunoblotting analysis revealed a marked decrease in HDAC1 and HDAC2 protein levels in cells infected with either HSV-1 or PRV, whereas the expression of HDAC4, HDAC6, and HDAC11 remained unchanged (Fig. 1A, B). In contrast, qRT-PCR results showed no alterations in HDAC1 and HDAC2 mRNA levels (Fig. 1C, D), suggesting that their depletion is regulated at the post-translational level.

To assess the functional impact of HDAC1/2 reduction, we examined global histone acetylation patterns. Site-specific immunoblotting demonstrated elevated acetylation at multiple lysine residues, including H3K9, H3K27, H3K56, H4K8, and H4K12, in HSV-1-infected HeLa cells (Fig. 1E). A similar hyperacetylation profile was observed in PRV-infected 3D4/21 cells and in murine liver tissues infected with HSV-1 (Fig. 1F, G). Next, we assessed the effect of HDAC1/2 knockdown on global histone acetylation and observed significantly elevated acetylation at multiple evolutionarily conserved lysine residues—including H3K9, H3K27, H3K56, H4K8, and H4K12—consistent with genome-wide histone hyperacetylation (Fig. H). Together, these findings indicate that HSV-1 selectively degrades class I HDACs, resulting in widespread histone hyperacetylation that fosters a chromatin state conducive to viral replication.

HSV-1 infection induces DDR through HDAC1/2 depletion and histone hyperacetylation

Given that excessive histone acetylation can destabilize chromatin structure, we sought to elucidate the mechanism by which this epigenetic modification activates the DDR pathway. Accumulating evidence underscores the pivotal role of histone modifications in maintaining genomic stability, with dynamic changes in chromatin architecture being intimately associated with DDR initiation. To determine whether HSV-1 infection induces DDR activation, we evaluated the phosphorylation of γ-H2AX, a well-established marker of DNA double-strand breaks. Immunofluorescence microscopy revealed a significant increase in γ-H2AX foci in cells infected with HSV-1 or PRV (Fig. 2A-C). Comet assays (single-cell gel electrophoresis) quantify DNA fragmentation, with an increased tail moment reflecting elevated levels of DNA damage—findings that further corroborate enhanced DNA fragmentation under these experimental conditions (Fig. 2D–G).Given the central role of ATM/ATR signaling in the DDR, we proceeded to examine the activation of key checkpoint kinases. Immunoblotting analysis confirmed phosphorylation of ATM, ATR, Chk1, Chk2, H2AX, and RAD51 in HSV-1-infected HeLa cells and 3D4/21 cells (Fig. 2H, I). Subsequently, we assessed the effect of HDAC1 knockdown on the DDR pathway and found that HDAC1-depleted HeLa cells exhibited reduced phosphorylation of ATM, ATR, and H2AX(Fig. 2J), providing initial evidence that HSV-1 infection promotes DDR activation through downregulation of HDAC1 expression.

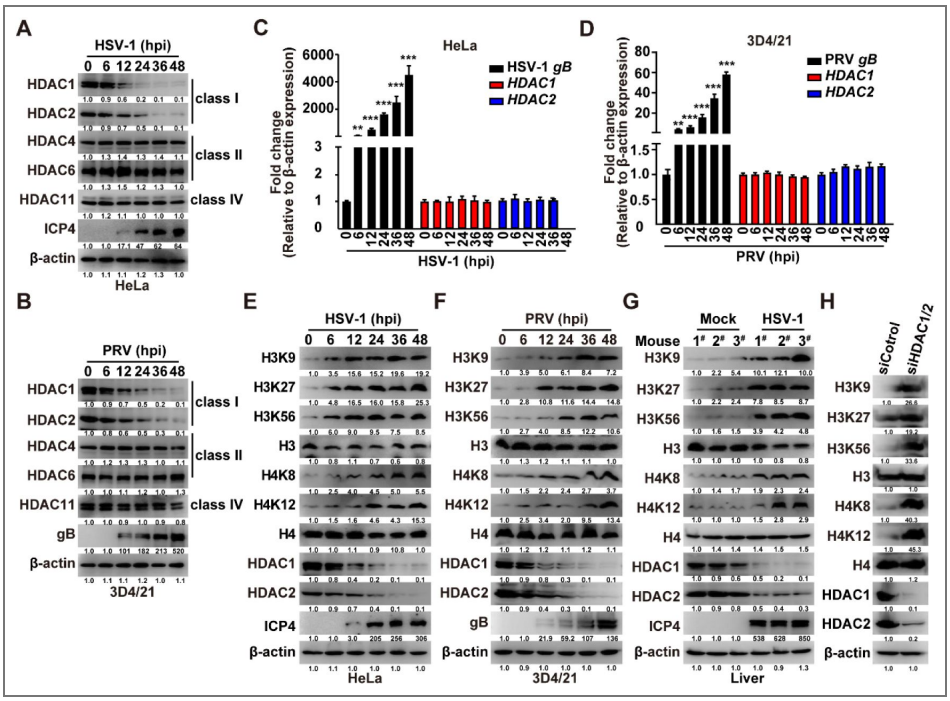

Figure 1. Viral infection induces degradation of class I HDACs and hyperacetylation of histones H3 and H4.

(A) Immunoblotting analysis of the indicated HDACs in HeLa cells infected with HSV-1 (MOI = 1) for the indicated time points. (B) Immunoblotting analysis of the indicated HDACs in 3D4/21 cells infected with PRV-QXX (MOI = 1) for the indicated time points. (C and D) qRT-PCR analysis of *HDAC1* and *HDAC2* mRNA levels, normalized to β-actin expression, in HeLa cells infected with HSV-1 (C) or 3D4/21 cells infected with PRV-QXX (D) (MOI = 1). Data are mean ± SEM; n = 3. $^{**}P < 0.01$, $^{***}P < 0.001$. (E) Immunoblotting of the indicated proteins in HeLa cells from infected with HSV-1 (MOI = 1) for the indicated time points. (F) Immunoblotting of the indicated proteins in 3D4/21 cells from infected with PRV-QXX (MOI = 1) for the indicated time points. (G) Immunoblotting analysis of the indicated proteins in liver tissues from mice mock-infected or infected with HSV-1 (1×10^6 pfu per mouse) at 5 days post-infection (n = 3). (H) Immunoblotting of the indicated proteins in HeLa cells transfected with siControl or siHDAC1/2.

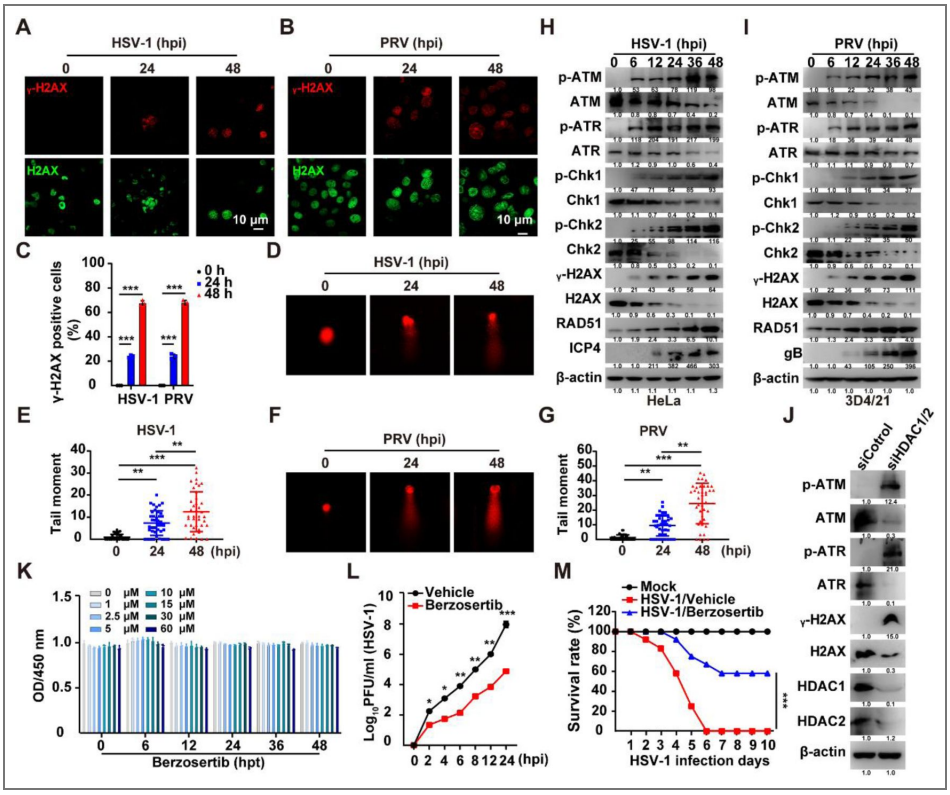

Figure 2. Viral infection triggers chromatin dysfunction and DDR activation via HDAC degradation.

(A, B and C) Immunofluorescence staining of γ-H2AX (red) and H2AX (green) in HSV-1-infected HeLa cells (A) or PRV-infected 3D4/21 cells (B) (MOI = 1). Panel C presents the quantitative analysis of γ-H2AX foci intensity or nuclear fluorescence signal derived from panels A and B. Scale bars: 10 μm. Data are mean ± SEM; n = 100 cells/group. ***$P < 0.001$. (D and E) Comet assay assessing DNA damage in HeLa cells infected with HSV-1 (MOI = 1). Data are mean ± SEM; n = 40 cells/group. **$P < 0.01$, ***$P < 0.001$. (F and G) Comet assay assessing DNA damage in 3D4/21 cells infected with PRV (MOI = 1) at the indicated time points. Data are mean ± SEM; n = 40 cells/group. **$P < 0.01$, ***$P < 0.001$. (H and I) Immunoblotting analysis of DDR markers (p-ATM, p-ATR, p-Chk1, p-Chk2, γ-H2AX) and viral ICP4/EP0 in HSV-1-infected HeLa cells (G) or PRV-QXX-infected 3D4/21 cells (H) (MOI = 1). (J) Immunoblotting analysis of DDR markers (p-ATM, p-ATR, γ-H2AX) and HDAC1/HDAC2 in HeLa cells transfected with siHDAC1/2. (K) HeLa cells were treated with vehicle and Berzosertib (0-60 μM) for 0–48 h. Cell proliferation was analyzed by CCK-8 assay. ns, no significance. (L) Viral titers in HSV-1-infected HeLa cells (MOI = 2) treated with berzosertib (50 nM) or vehicle. Data are mean ± SEM; n = 3. *$P < 0.05$, **$P < 0.01$, ***$P < 0.001$ (M) Survival curves of HSV-1-infected mice (1×10^6 PFU/mouse) treated with berzosertib (20 mg/kg) or vehicle (n = 12/group), ***$P < 0.001$.

Next, we pharmacologically validated the functional relevance of ATR in HSV-1 replication using Berzosertib, a selective and clinically advanced ATR inhibitor. CCK-8 assays confirmed that the concentration of Berzosertib used (100 nM) did not significantly affect HeLa cell viability or proliferation over 48 hours (Fig. 2K), yet it markedly reduced viral titers in plaque assays (Fig. 2L). Collectively, these findings demonstrate that HSV-1 infection activates the DDR, likely through degradation of HDAC1 and HDAC2 and the resulting histone hyperacetylation. This virus-triggered DDR activation highlights the profound disruption of host chromatin homeostasis and genomic integrity by HSV-1.

HSV-1 promotes the ubiquitin-proteasome degradation of HDAC1/2

To elucidate the mechanism responsible for HDAC1/2 degradation, we focused on their post-translational regulation. Since HDAC1/2 mRNA levels were unchanged after infection, we hypothesized that the reduction in HDAC1/2 protein is mediated through enhanced proteolytic degradation. To identify the relevant degradation pathway, HSV-1-infected HeLa cells were treated with either the proteasome inhibitor MG-132 or autophagy inhibitors (3-MA and chloroquine). Immunoblotting analysis indicated that only MG-132 rescued HDAC1/2 protein levels (Fig. 3A), confirming that degradation occurs primarily via the proteasomal pathway.

To examine whether HSV-1 infection induced ubiquitination of HDAC1, endogenous immunoprecipitation assays were performed, which revealed increased ubiquitination of HDAC1 following infection (Fig. 3B). Subsequent ubiquitination assays using wild-type (WT), K48-only, and K63-only ubiquitin mutants demonstrated that HDAC1 undergoes K63-linked—but not K48-linked—polyubiquitination (Fig. 3C). Using a series of HDAC1 truncation mutants, we mapped the ubiquitination site to the N-terminal region (amino acids 1–100) (Fig. 3D–F). Site-directed mutagenesis further identified lysine 74 (K74) as the critical residue required for ubiquitination (Fig. 3G–I). Sequence alignment showed that HDAC2 K75 corresponds to HDAC1 K74 (Fig. 3J), and a K75R mutation in HDAC2 similarly abolished ubiquitination (Fig. 3J).

To further validate the role of HDAC1 K74, we first overexpressed HDAC1 WT and HDAC1 K74R and assessed phosphorylation of ATM, ATR, and H2AX; results showed that HDAC1 K74R overexpression suppressed HSV-1–induced DDR signaling(Fig. 3K). Furthermore, RT–PCR analysis revealed that overexpression of both HDAC1 WT and HDAC1 K74R inhibited HSV-1 ICP0,ICP8 and gB expression, but HDAC1 WT exerted a significantly stronger inhibitory effect (Fig. 3L). Consistently, HDAC1 K74R overexpression reduced viral titers in plaque assays (Fig. 3M). Together, these results indicate that HSV-1 infection promotes K63-linked polyubiquitination of HDAC1/2 at conserved lysine residues, ultimately leading to their proteasomal degradation. Together, these results indicate that HSV-1 infection promotes K63-linked polyubiquitination of HDAC1/2 at conserved lysine residues, ultimately leading to their proteasomal degradation.

MDM2 functions as the E3 ligase mediating HDAC1/2 ubiquitination and degradation

Having established the occurrence of K63-linked ubiquitination (Fig. 3), we next sought to identify the E3 ubiquitin ligase responsible. An RNAi screen targeting candidate E3 ligases revealed MDM2 as the principal mediator of HDAC1/2 degradation. Knockdown of MDM2—but not of PIRH2, KCTD11, CHFR, UHRF1, or TRIM46—effectively prevented HDAC1/2 depletion (Fig. 4A, B). Co-IP assay further confirmed an enhanced interaction between HDAC1 and MDM2 following HSV-1 infection (Fig. 4C).

To characterize this interaction, we focused on the RING finger domain of MDM2, which is essential for its E3 ligase activity. Co-IP analysis demonstrated that HSV-1 infection promoted binding between FLAG-HDAC1 and EGFP-MDM2, but not with a RING-deleted mutant (EGFP-MDM2ΔRING) (Fig. 4D), indicating that the interaction was RING domain-dependent. To identify the region within HDAC1 required for binding, HeLa cells were co-transfected with EGFP-MDM2

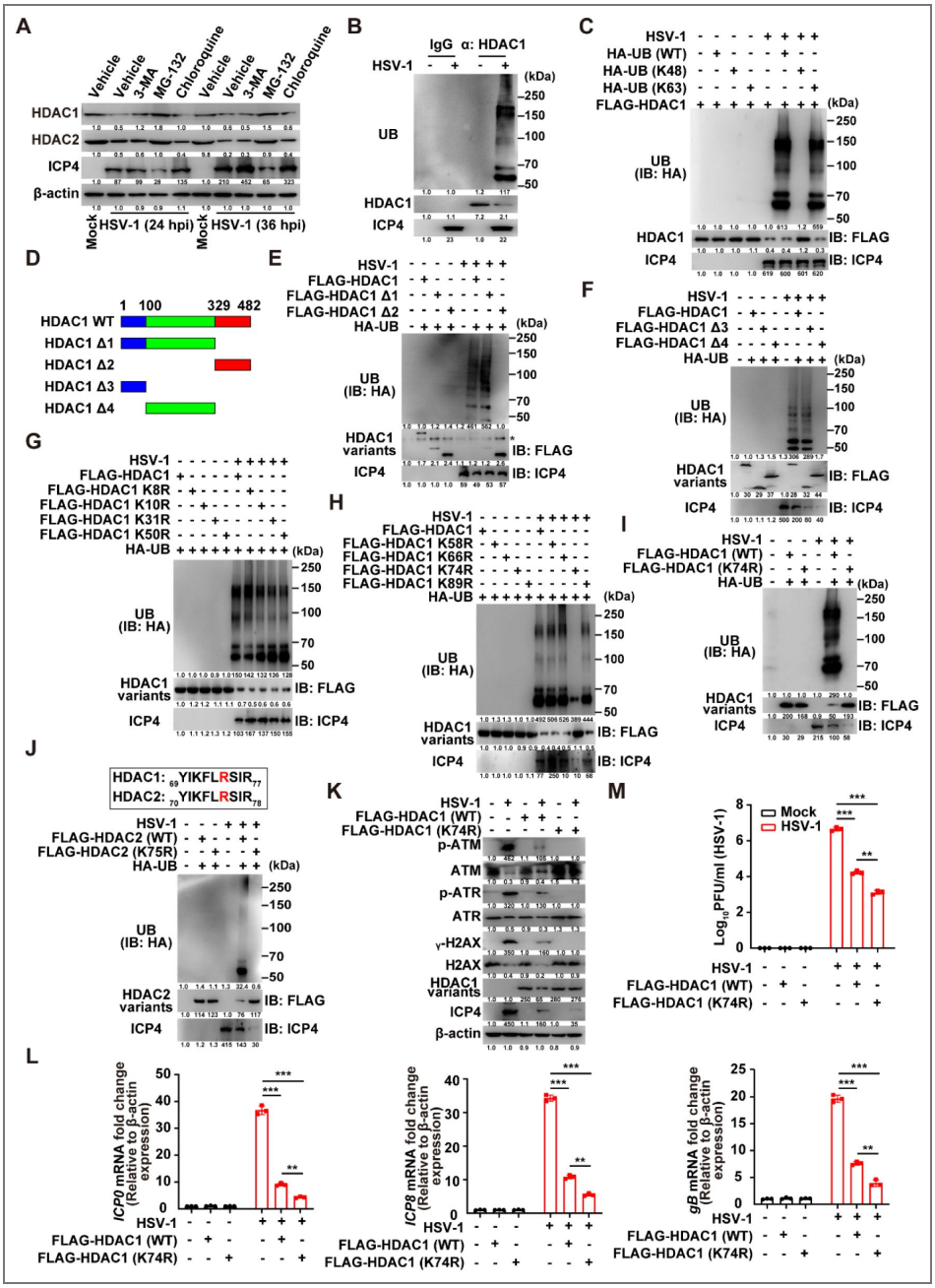

Figure 3. Viral infection induces K63-linked ubiquitination of HDAC1/2.

(A) Immunoblotting analysis of the indicated proteins in HeLa cells either mock-infected or infected with HSV-1 (MOI = 1), treated with vehicle, 3-MA (10 μM), MG-132 (10 μM), or chloroquine (10 μM) for the indicated times. (B) Ubiquitination assay of HDAC1 in HeLa cells either mock-infected or infected with HSV-1 (MOI = 1) at 24 hpi. (C) Ubiquitination assay of FLAG-HDAC1 in HeLa cells transfected with HA-ubiquitin variants (WT, K48, K63), and either mock-infected or infected with HSV-1 (MOI = 1) at 24 hpi. (D) Schematic representation of HDAC1 deletion mutants. (E-I) Ubiquitination assays of FLAG-HDAC1 mutant variants in HeLa cells either mock-infected or infected with HSV-1 (MOI = 1) at 24 hpi. (J) Ubiquitination assays of FLAG-HDAC2 variants (WT and K75R) in HeLa cells either mock-infected or infected with HSV-1 (MOI = 1) at 24 hpi. (K) Immunoblotting analysis of the indicated proteins in HeLa cells transfected with FLAG-HDAC1 and FLAG-HDAC1 (K74R), and either mock-infected or infected with HSV-1 (MOI = 1) at 24 hpi. (L) qRT-PCR analysis of HSV-1 *ICP0*,*ICP8* and *gB* mRNA levels, normalized to β-actin expression, in HeLa cells transfected with FLAG-HDAC1 and FLAG-HDAC1 (K74R), and either mock-infected or infected with HSV-1 (MOI = 1) at 24 hpi. Data are mean ± SEM; n = 3. ns > 0.05,*P < 0.05,**P < 0.01, ***P < 0.001. (M) Viral titer analysis in HeLa cells transfected with FLAG-HDAC1 or FLAG-HDAC1 (K74R), and either mock-infected or infected with HSV-1 (MOI = 1) at 24 hpi. Data are mean ± SEM; n = 3. **P < 0.01, ***P < 0.001.

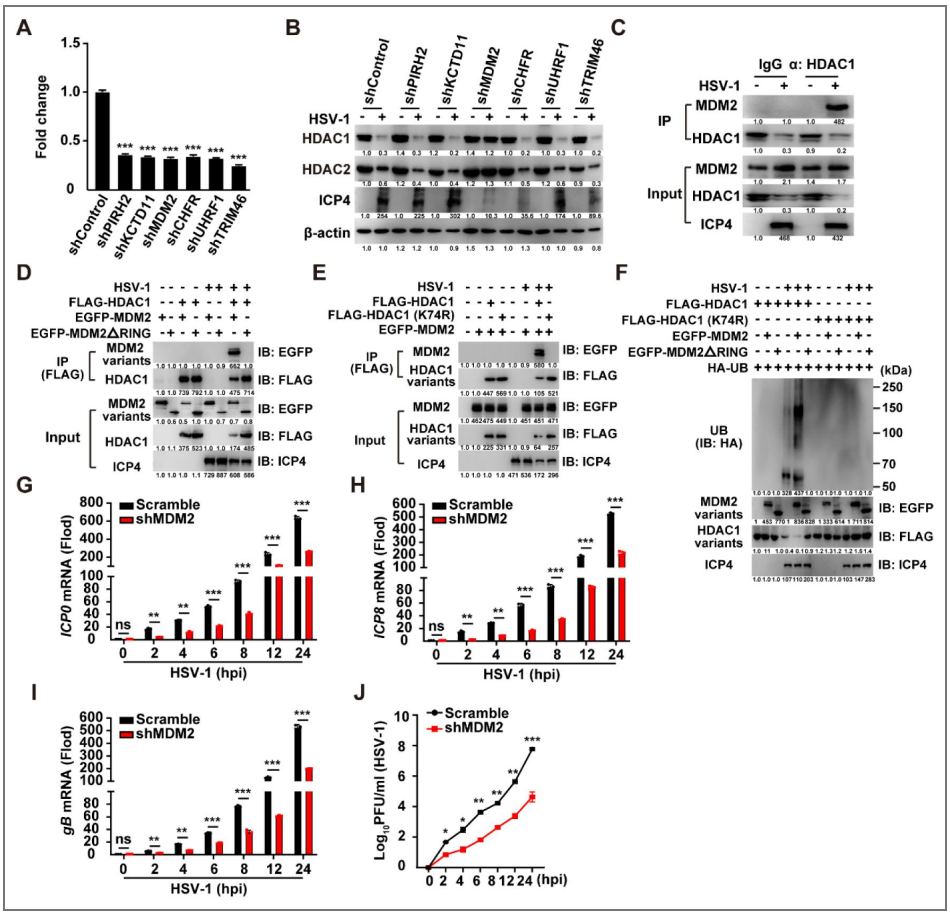

Figure 4. MDM2 mediates viral-induced HDAC1/2 degradation via K74/K75 ubiquitination.

(A) qRT-PCR analysis validation of E3 ligase knockdown efficiency (shPIRH2, shKCTD11, shMDM2, shCHFR, shUHRF1, shTRIM46) in HeLa cells. Data are mean ± SEM; n = 3. ***P < 0.001. (B) Immunoblotting analysis of HDAC1/2 stability in E3 ligase-knockdown HeLa cells infected with HSV-1 (MOI = 1). (C) Co-IP assay of endogenous HDAC1-MDM2 interaction in HSV-1-infected HeLa cells (MOI = 1; 24 hpi). (D) Co-IP assay of FLAG-HDAC1 with EGFP-MDM2 (WT or ΔRING) in HSV-1-infected HeLa cells (MOI = 1; 24 hpi). (E) Co-IP assay of FLAG-HDAC1 (WT or K74R) with EGFP-MDM2 in HSV-1-infected HeLa cells (MOI = 1; 24 hpi). (F) Ubiquitination assays of FLAG-HDAC1 (WT or K74R) co-expressed with EGFP-MDM2 (WT or ΔRING) in HSV-1-infected HeLa cells (MOI = 1; 24 hpi). (G-I) qRT-PCR analysis of HSV-1 *ICP0 (H)*,*ICP8 (I)*and *gB (J)* mRNA levels, normalized to β-actin expression, in Scramble and shMDM2 HeLa cells, and either mock-infected or infected with HSV-1 (MOI = 1) at 24 hpi. Data are mean ± SEM; n = 3. ns > 0.05,*P < 0.05,**P < 0.01, ***P < 0.001. (J) Viral titer analysis in Scramble and shMDM2 HeLa cells, either mock-infected or infected with HSV-1 (MOI = 2) at 24 hpi. Data are mean ± SEM; n = 3. **P < 0.01, ***P < 0.001.

and either FLAG-HDAC1 or the ubiquitination-resistant mutant FLAG-HDAC1 K74R. Infection with HSV-1 failed to induce binding between EGFP-MDM2 and the K74R mutant (Fig. 4E), underscoring the essential role of lysine 74 in mediating MDM2-dependent ubiquitination.

Ubiquitination assay further revealed that overexpression of EGFP-MDM2ΔRING did not enhance HSV-1-induced ubiquitination or degradation of HDAC1 (Fig. 4F). Similarly, the FLAG-HDAC1 K74R mutant remained resistant to ubiquitination under all experimental conditions (Fig. 4F). To further validate the role of MDM2, we performed MDM2 knockdown in infected cells; RT–PCR analysis showed that MDM2 knockdown significantly suppressed HSV-1 *ICP0*, *ICP8*, and *gB* mRNA transcription (Fig. 4G–I), and reduced viral titers in plaque assays (Fig. 4J). Collectively, these results demonstrate that HSV-1 induces HDAC1/2 degradation through MDM2-mediated K63-linked ubiquitination.

HSV-1 triggers cytoplasmic translocation of HDAC1 to facilitate its degradation

To elucidate the mechanisms by which HSV-1 induces HDAC degradation, we systematically analyzed the subcellular localization of HDAC1. In mock-infected HeLa cells, HDAC1 was predominantly nuclear; however, HSV-1 infection triggered a pronounced translocation of HDAC1 to the cytoplasm (Fig. 5B). This redistribution was completely abolished by treatment with leptomycin B (LMB), a specific inhibitor of CRM1-mediated nuclear export (Fig. 5B). At the same time, CCK-8 assay showed that LMB had no significant effect on cell proliferation (Fig. 5A).

To determine whether translocation is functionally linked to degradation, we conducted cycloheximide (CHX) chase assays. Degradation of both HDAC1 and HDAC2 began approximately 12 hours after CHX treatment and was markedly accelerated by HSV-1 infection (Fig. 5D). Importantly, LMB treatment restored degradation kinetics to levels comparable to those in mock-infected cells (Fig. 5B). Moreover, under LMB treatment, HSV-1 was unable to induce ubiquitination of endogenous HDAC1 (Fig. 5E). To further validate the subcellular site of HDAC1 ubiquitination, we performed nucleocytoplasmic fractionation followed by immunoblotting; results showed that HSV-1–induced ubiquitination of endogenous HDAC1 occurs specifically in the cytoplasm (Fig. 5F).

We further demonstrated that nuclear export and subsequent proteasomal degradation of HDAC1 are strictly dependent on the E3 ubiquitin ligase MDM2. HSV-1 infection induces CRM1-dependent ubiquitination of endogenous HDAC1, thereby establishing CRM1-mediated nuclear export as an essential prerequisite for MDM2-catalyzed HDAC1 degradation (Fig. 5G, H). Consistent with this, immunoblotting analysis revealed that LMB significantly suppressed HSV-1–induced phosphorylation of p53 and γH2AX (Fig. 5I). Notably, LMB treatment-by inhibiting CRM1-dependent nuclear export and thereby preventing HDAC1 degradation—markedly impaired HSV-1 replication (Fig. 5F). To rigorously test whether HDAC1 nuclear export is the critical, rate-limiting step enabling its ubiquitination and degradation, we employed NESmapper to identify a canonical nuclear export signal (NES) in HDAC1 (residues 207–216). We then generated an HDAC1 ΔNES deletion mutant and performed functional rescue experiments in HDAC1-knockdown cells by reconstituting expression of HDAC1 WT, the ubiquitination-deficient mutant HDAC1 K74R, or FLAG-tagged HDAC1 ΔNES. Only HDAC1 WT fully restored the pro-viral phenotype associated with HDAC1 depletion; in contrast, neither HDAC1 K74R nor HDAC1 ΔNES rescued viral replication, and both exerted potent antiviral activity—significantly suppressing HSV-1 proliferation relative to controls (Fig. 5K). Collectively, these findings establish that HSV-1 co-opts the CRM1 nuclear export machinery to translocate HDAC1 to the cytoplasm, where it becomes accessible to MDM2 for ubiquitination and subsequent proteasomal degradation, thereby modulating host antiviral defense.

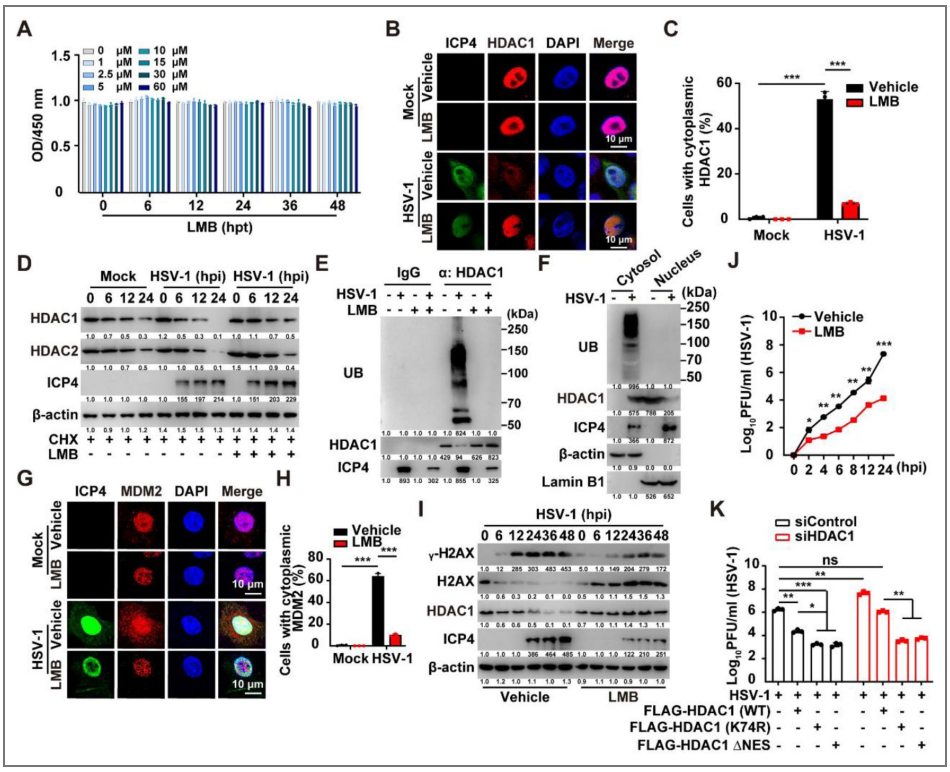

Figure 5. Cytoplasmic translocation enables MDM2-mediated HDAC1 degradation.

(A) HeLa cells were treated with vehicle and LMB (0-60 μM) for 0–48 h. Cell proliferation was analyzed by CCK-8 assay. ns, no significance. (B and C) Immunofluorescence staining of HDAC1 (red) and viral ICP4 (green) in HSV-1-infected HeLa cells (MOI = 1) ± leptomycin B (LMB; 10 nM; 24 h). Scale bar: 10 μm. (C) shows the quantitative analysis of (B), Data are mean ± SEM; n = 100. ***P < 0.001. (D) CHX chase assay measuring HDAC1/2 degradation kinetics in HSV-1-infected HeLa cells (MOI = 1) ± LMB (10 μM). (E) Ubiquitination assay of HDAC1 in HSV-1-infected HeLa cells (MOI = 1) ± LMB (10 μM; 24 h). (F) Immunoblotting analysis of ubiquitination in HDAC1 from cytosolic and nuclear fractions of HeLa cells infected with HSV-1. (G and H) Immunofluorescence analysis of MDM2 (red) and ICP4 (green) in HSV-1-infected HeLa cells (MOI = 1) ± LMB (10 μM; 24 h). Scale bar: 10 μm. (H) shows the quantitative analysis of (G), Data are mean ± SEM; n = 100. ***P < 0.001. (I) Immunoblotting analysis of DDR markers (γ-H2AX) and HDAC1/2 in HSV-1-infected HeLa cells (MOI = 1) ± LMB (10 μM). (J) Viral titers in HSV-1-infected HeLa cells (MOI = 2) ± LMB (10 μM). Data are mean ± SEM; n = 3. *P < 0.05, **P < 0.01, ***P < 0.001 (K) Viral titer analysis in HeLa cells transfected with siHDAC1 transfected with FLAG-HDAC1,FLAG-HDAC1 (K74R) or FLAG-HDAC1 ΔNES, infected with HSV-1 (MOI = 1) at 24 hpi. Data are mean ± SEM; n = 3. **P < 0.01, ***P < 0.001.

Discussion

HSV-1 manipulates host cellular pathways to facilitate its replication, latency, and reactivation[26]. In this study, we demonstrate that alphaherpesvirus targets class I histone deacetylases HDAC1 and HDAC2 for MDM2-mediated K63-linked polyubiquitination and subsequent proteasomal degradation. This degradation induces histone hyperacetylation, chromatin relaxation, and enhanced viral replication—revealing a mechanism through which alphaherpesvirus reprograms the host epigenetic landscape to optimize viral replication (Fig. 6).

In contrast, HSV-1 actively targets HDAC1 and HDAC2 for proteasomal degradation to facilitate lytic replication—a strategy that stands in marked contrast to human cytomegalovirus (HCMV), which relies on HDAC activity to maintain latency[27]. This divergence underscores a fundamental difference in epigenetic regulation among herpesviruses. Our data demonstrate that HSV-1–mediated HDAC1/2 degradation initiates as early as 4–6 hours post-infection, coinciding with the onset of immediate-early gene expression and preceding peak viral DNA synthesis. These findings support a context-dependent, dual functional role for HDAC1/2: their enzymatic activity helps enforce transcriptional silencing during latency, whereas their timely removal is essential for chromatin remodeling and efficient lytic gene expression.

We identified MDM2[28] as the principal E3 ubiquitin ligase responsible for ubiquitinating HDAC1 at lysine 74 and HDAC2 at lysine 75, leading to their proteasomal degradation. This mechanism is distinct from other E3 ligases, including PIRH2[29] and TRIM46[30]), and critically depends on the RING domain of MDM2[31]. While K63-linked ubiquitination is typically associated with non-proteolytic functions, our work establishes its novel role in mediating HDAC1/2 degradation—uncovering a previously unrecognized viral pathogenesis pathway. Targeting this axis using MDM2 inhibitors or inhibiting nuclear export of HDAC1/2 significantly restricts viral replication, suggesting that host-directed antiviral strategies may help overcome resistance to direct-acting agents[31].

Depletion of HDAC1/2 increases acetylation at histone residues associated with open chromatin and active transcription. Similar chromatin remodeling has been observed in other viral infections[32], underscoring its conserved role in viral gene regulation. Our results are consistent across multiple cell types, including HeLa, 3D4/21, and murine liver, emphasizing the central importance of HDAC1/2 suppression in HSV-1 biology. Notably, HDAC1/2 degradation activates DDR, as indicated by increased γ-H2AX foci and phosphorylation of ATM, ATR, Chk1, and Chk2. This aligns with previous reports that HSV-1 exploits DDR signaling to enhance replication[33–35]. Importantly, HDAC1/2 undergo CRM1-dependent nuclear export prior to degradation—a process inhibited by leptomycin B—highlighting the essential role of subcellular localization in viral manipulation of host proteins.

HSV-1–mediated HDAC1/2 degradation likely supports viral replication through multiple mechanisms, including evasion of nuclear antiviral sensors and stimulation of viral gene expression. Targeting the MDM2–HDAC1/2 axis represents a promising antiviral strategy. MDM2 inhibitors reduce HSV-1 titers [36], suggesting that modulating ubiquitination pathways could complement existing therapies. Beyond herpesviruses, the MDM2–HDAC axis may be exploited by other DNA viruses that manipulate chromatin and DDR[32], indicating a possible common host vulnerability. However, broad HDAC inhibition may unintentionally enhance viral replication, underscoring the need for targeted therapeutic approaches[37].

This study primarily employed in vitro models (HeLa cells), which lack the neuronal environment essential for studying HSV-1 latency. Future work should validate these findings in primary neurons and trigeminal ganglia [38]. Additional studies are also needed to determine whether HDAC1/2 degradation occurs during reactivation or is limited to lytic infection[7], and to explore the interplay between HDAC degradation, viral tegument proteins, and host stress responses. In vivo evaluation of inhibitors targeting the MDM2/HDAC1–2 pathway will be crucial for assessing their therapeutic potential.

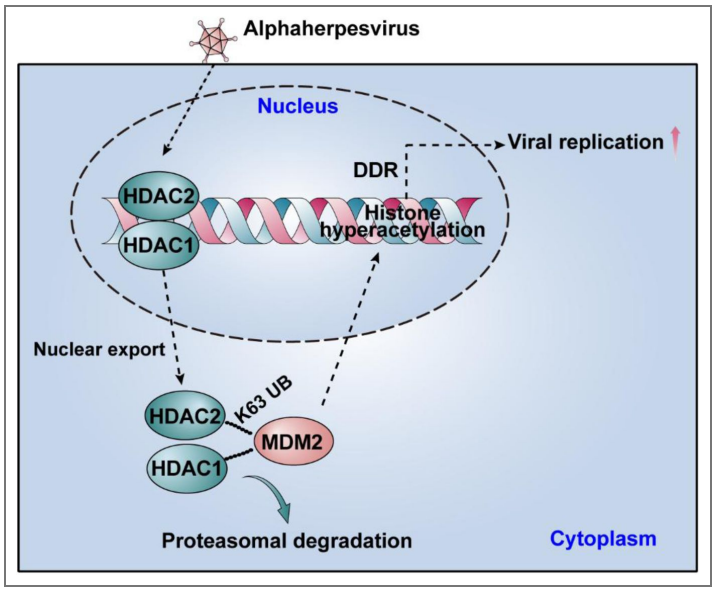

Figure 6. **A schematic model showing the targeted cytosolic degradation of class I histone deacetylases is essential for efficient alphaherpesvirus replication.**

Genes	Forward (5′-3′)	Reverse (5′-3′)
Human Q-HDAC1	CATCGCTGTGAATTGGGCTG	CCCTCTGGTGATACTTTAGCAGT
Human Q-HDAC2	TGGCCTTTCTGAGCTGATTT	AGCCACTGAAACAAGACTTCA
Human Q-β-actin	CCTTGCACATGCCGGAG	GCACAGAGCCTCGCCTT
Sus Q-β-actin	CTGAACCCCAAAGCCAACCGT	TTCTCCTTGATGTCCCGCACG
HSV-1-gB	GGACATCAAGGCGGAGAACA	TTCTCCTTGAAGACCACCGC
HSV-1-ICP0	TCTGCATCCCGTGCATGAAAAC	TCACGCCCACTATCAGGTACAC
HSV-1-ICP4	ATCGCATCGGAA AGGGACACG	CCAAGGTGCTTACCCGTGCAA A
siHDAC1	GGCUAGUGUUAUAGAUUAAGC	UUAAUCUAUAACACUAGCCUU
siHDAC2	GGUCAAUAAGACCAGAUAACA	UUAUCUGGUCUUAUUGACCGU
siControl	UUCUCCGAACGUGUCACGUTT	ACGUGACACGUUCGGAGAATT
PRV-gB	CTCGCCATCGTCAGCAA	GCTGCTCCTCCATGTCCTT
Sus Q-HDAC1	TGACGAGTCCTATGAGGCCA	CAAACTCCACACACTTGGCG
Sus Q-HDAC2	CCCCATAAAGCCACTGCTGA	AGCCACCAGTTGAAAGCTGA
Human Q-PIRH2	TATCCTGGGGGAAGGATCGG	TCATGACACAAGCGGCAAGT
Human sh-PIRH2	AATGTAACTTATGCCTAGCTA	TAGCTAGGCATAAGTTACATT
Human sh-KCTD11	GGCACATCCTCAATTTCCTGA	TCAGGAAATTGAGGATGTGCC
Human Q-KCTD11	GATGTAGATGTCAGCCCCCG	GTGCAGAAAAGGTTGGCTCG
Human sh-MDM2	GCCAGAGTGAGTCAGACAAGT	ACTTGTCTGACTCACTCTGGC
Human Q-MDM2	ACCCTGGTTAGACCAAAGCC	TGGCACGCCAAACAAATCTC
Human sh-CHFR	GCAACCAGAGGTTTGACATGG	CCATGTCAAACCTCTGGTTGC
Human Q-CHFR	TGTGTTCCATGGGACCAAAGAT	ACGTCGATGTTGATGGCTGT
Human sh-UHRF1	GCCAGAGTGAGTCAGACAAGT	ACTTGTCTGACTCACTCTGGC
Human Q-UHRF1	AACAGCTCCTGGATCTTCCG	GGTTTCATCGCCATCCCCA
Human sh-TRIM46	GGTGAGGATATGCAGACCTTC	GAAGTCTGCATATCCTCACC
Human Q-TRIM46	ACGGCGAATACAGTGAAG	GCTGGTCCTTGCTGATAG

Table S1. **List of shRNAs and primers used in this study.**

Data availability

The datas that support the findings of this study are openlyavailable in "Mendeley Data, V3" at *https://data.mendeley.com/datasets/yg5fgtvxzk/3*, doi: *10.17632/yg5fgtvxzk.3*.

Additional information

Author contributions

Sheng-Li Ming and Meng-Hua Du : Data curation, Formal analysis, Investigation, Methodology, Validation, Visualization, Writing – original draft; Jia-Ming Yang: Data curation, Formal analysis, Investigation, Validation; Ya-Di Guo: Data curation, Formal analysis, Investigation, Validation, Visualization; Jia-Jia Pan: Data curation, Formal analysis, Investigation, Methodology, Visualization; Wei-Fei Lu: Data curation, Formal analysis, Investigation; Jiang Wang: Methodology, Visualization, Project administration, Supervision, Writing – review & editing; Lei Zeng and Bei-Bei Chu: Conceptualization, Data curation, Funding acquisi-tion, Investigation, Methodology, Project administration, Resources, Supervision, Validation, Writing – original draft, Writing – review & editing.

Ethics statement

All procedures involving animals in this study received ethical approval from the Institutional Animal Care and Use Committee (IACUC) of Henan Agricultural University (Permit Number: HNND2020031008). This research was performed in accordance with the regulations specified in the Guide for the Care and Use of Laboratory Animals established by the Ministry of Science and Technology of China

Funding

This research was supported by grants from the National Key R&D Program of China (2021YFD1301200 and 2023YFD1801600), the China Postdoctoral Science Foundation (2025M770267, GZC20240430).

Declaration of generative AI and AI-assisted technologies in the writing process

This study affirms that neither generative artificial intelligence nor any other AI-assisted technologies were employed in the preparation of this manuscript.

Funding

Funder	Grant reference number	Author
MOST | National Key Research and Development Program of China (NKPs)	2021YFD1301200	Bei-Bei Chu
National Key Project for Research on Transgenic Biology	2023YFD1801600	Bei-Bei Chu
China Postdoctoral Science Foundation (中国博士后科学基金会职)	2025M770267	Shengli Ming
China Postdoctoral Science Foundation (中国博士后科学基金会职)	GZC20240430	Shengli Ming

Author ORCID iDs

Sheng-Li Ming: https://orcid.org/0000-0002-7505-6143
Bei-Bei Chu: https://orcid.org/0000-0003-2961-4754

References

1. **Charlotte J,** Manale H, Nicky J W, Katherine Me T, Laith J A-R, Sami L G, et al. (2020) Herpes simplex virus: global infection prevalence and incidence estimates, 2016. *Bull World Health Organ* **98** https://doi.org/10.2471/blt.19.237149 | PubMed
2. **Shu F,** Yongzhen L, Yu Z, Zhenfeng S, Zhuxi C, Charles B, et al. (2023) Mechanistic insights into the role of herpes simplex virus 1 in Alzheimer's disease. *Front Aging Neurosci* **15** https://doi.org/10.3389/fnagi.2023.1245904 | PubMed
3. **Damon J D,** Ning Q, Jonathan P G (2016) Neuroinflammation: the devil is in the details. *J Neurochem* https://doi.org/10.1111/jnc.13607 | PubMed
4. **Modi S,** Mahajan A, Dharaiya D, Varelas P, Mitsias P (2017) Burden of herpes simplex virus encephalitis in the United States. *J Neurol* **264** https://doi.org/10.1007/s00415-017-8516-x | PubMed
5. **Saba A,** Francesca B (2010) Targeting cyclooxygenases-1 and -2 in neuroinflammation: Therapeutic implications. *Biochimie* **93** https://doi.org/10.1016/j.biochi.2010.09.009 | PubMed
6. **Orhan A,** Oliver U, Carmen I-D, Robert N, Frauke Z (2007) Neuronal damage in brain inflammation. *Arch Neurol* **64** https://doi.org/10.1001/archneur.64.2.185 | PubMed
7. **David M K,** Anna C (2008) Chromatin control of herpes simplex virus lytic and latent infection. *Nat Rev Microbiol* **6** https://doi.org/10.1038/nrmicro1794 | PubMed
8. **Luis M S,** MiYao H, Esteban Flores C, Kairui S (2021) Chromatin-mediated epigenetic regulation of HSV-1 transcription as a potential target in antiviral therapy. *Antiviral Res* **192** https://doi.org/10.1016/j.antiviral.2021.105103 | PubMed
9. **Te D,** Guoying Z, Shaniya K, Haidong G, Bernard R (2010) Disruption of HDAC/CoREST/REST repressor by dnREST reduces genome silencing and increases virulence of herpes simplex virus. *Proc Natl Acad Sci U S A* **107** https://doi.org/10.1073/pnas.1010741107 | PubMed
10. **Rui F,** Fei C, Zhenghong D, Di H, Andrew J B, Erin A C, et al. (2012) LSD2/KDM1B and its cofactor NPAC/GLYR1 endow a structural and molecular model for regulation of H3K4 demethylation. *Mol Cell* **49** https://doi.org/10.1016/j.molcel.2012.11.019 | PubMed
11. **Guoying Z,** Te D, Bernard R (2013) HSV carrying WT REST establishes latency but reactivates only if the synthesis of REST is suppressed. *Proc Natl Acad Sci U S A* **110** https://doi.org/10.1073/pnas.1222497110 | PubMed
12. **Maria S,** Asifa A (2022) Modulation of cellular processes by histone and non-histone protein acetylation. *Nat Rev Mol Cell Biol* **23** https://doi.org/10.1038/s41580-021-00441-y | PubMed
13. **Patrick L,** Joëlle T, Pascale T, Cécile C, Saadi K, Alberto L E (2004) Functional interaction between class II histone deacetylases and ICP0 of herpes simplex virus type 1. *J Virol* **78** https://doi.org/10.1128/jvi.78.13.6744-6757.2004 | PubMed
14. **Georges H,** Daniel W (2010) Histone deacetylases in viral infections. *Clin Epigenetics* **1** https://doi.org/10.1007/s13148-010-0003-5 | PubMed
15. **Hao-Ming C,** Matthew P, Michelle H, Charles M R, Bryan R G W, Isabelle M, et al. (2004) Induction of interferon-stimulated gene expression and antiviral responses require protein deacetylase activity. *Proc Natl Acad Sci U S A* **101** https://doi.org/10.1073/pnas.0400567101 | PubMed
16. **Isabelle J M,** Hao-Ming C, David E L (2018) HDAC stimulates gene expression through BRD4 availability in response to IFN and in interferonopathies. *J Exp Med* **215** https://doi.org/10.1084/jem.20180520 | PubMed
17. **Inna N,** Curt M H (2003) Interferon-stimulated transcription and innate antiviral immunity require deacetylase activity and histone deacetylase 1. *Proc Natl Acad Sci U S A* **100** https://doi.org/10.1073/pnas.2433987100 | PubMed
18. **Amanda J G,** Hanna G B, Benjamin A D, Ileana M C (2013) Histone deacetylases in herpesvirus replication and virus-stimulated host defense. *Viruses* **5** https://doi.org/10.3390/v5071607 | PubMed

19. **Sutapa R,** Chang L, Tieying H, Istvan B, Allan R B (2008) Requirement of histone deacetylase1 (HDAC1) in signal transducer and activator of transcription 3 (STAT3) nucleocytoplasmic distribution. *Nucleic Acids Res* **36** https://doi.org/10.1093/nar/gkn419 | PubMed

20. **Xue L,** Xiangrong L, Pengpeng H, Facai Z, Juanjuan K D, Ying K, et al. (2024) Acetylation of TIR domains in the TLR4-Mal-MyD88 complex regulates immune responses in sepsis. *EMBO J* **43** https://doi.org/10.1038/s44318-024-00237-8 | PubMed

21. **Oriana M,** Natalie K H, Laura Z, Silvia C, Richard S, Stefan Z, et al. (2024) Inflammation-driven NF-κB signaling represses ferroportin transcription in macrophages via HDAC1 and HDAC3. *Blood* **145** https://doi.org/10.1182/blood.2023023417 | PubMed

22. **Meiyu S,** Xiaoqing Z, Jiamei S, Hongyan D, Xin H, Qiao Y, et al. (2025) Saikosaponin b1 Attenuates Liver Fibrosis by Blocking STAT3/Gli1 Interaction and Inducing Gli1 Degradation. *Exploration (Beijing)* **5** https://doi.org/10.1002/exp.70000 | PubMed

23. **Prashanth Thevkar N,** Matloob H (2016) Influenza A Virus Dysregulates Host Histone Deacetylase 1 That Inhibits Viral Infection in Lung Epithelial Cells. *J Virol* **90** https://doi.org/10.1128/jvi.00126-16 | PubMed

24. **Jiang W,** Guo-Li L, Sheng-Li M, Chun-Feng W, Li-Juan S, Bing-Qian S, et al. (2020) BRD4 inhibition exerts anti-viral activity through DNA damage-dependent innate immune responses. *PLoS Pathog* **16** https://doi.org/10.1371/journal.ppat.1008429 | PubMed

25. **Leong J,** Husain M (2024) HDAC1 and HDAC2 Are Involved in Influenza A Virus-Induced Nuclear Translocation of Ectopically Expressed STAT3-GFP. *Viruses* **17** https://doi.org/10.3390/v17010033 | PubMed

26. **Bernard R,** Richard J W (2013) An inquiry into the molecular basis of HSV latency and reactivation. *Annu Rev Microbiol* **67** https://doi.org/10.1146/annurev-micro-092412-155654 | PubMed

27. **Jane C M,** Wolfgang F, Eric V, John H S (2002) Control of cytomegalovirus lytic gene expression by histone acetylation. *EMBO J* **21** https://doi.org/10.1093/emboj/21.5.1112 | PubMed

28. **Honda R,** Tanaka H, Yasuda H (1998) Oncoprotein MDM2 is a ubiquitin ligase E3 for tumor suppressor p53. *FEBS Lett* **420** https://doi.org/10.1016/s0014-5793(97)01480-4 | PubMed

29. **Alexandra D,** Olga F, Sergey P, Ivan N, Oleg S, Nickolai A B (2022) The Role of E3 Ligase Pirh2 in Disease. *Cells* **11** https://doi.org/10.3390/cells11091515 | PubMed

30. **Jicheng T,** Xufeng P, Yong C, Yuzhou S, Chunyu J (2022) TRIM46 activates AKT/HK2 signaling by modifying PHLPP2 ubiquitylation to promote glycolysis and chemoresistance of lung cancer cells. *Cell Death Dis* **13** https://doi.org/10.1038/s41419-022-04727-7 | PubMed

31. **Mark W,** Yunyuan V W, Geoffrey M W (2010) The p53 orchestra: Mdm2 and Mdmx set the tone. *Trends Cell Biol* **20** https://doi.org/10.1016/j.tcb.2010.01.009 | PubMed

32. **Lieberman PM** (2016) Epigenetics and Genetics of Viral Latency. *Cell Host Microbe* **19** https://doi.org/10.1016/j.chom.2016.04.008 | PubMed

33. **Max E M,** David M K (2021) Herpes Simplex Virus 1 Manipulates Host Cell Antiviral and Proviral DNA Damage Responses. *mBio* **12** https://doi.org/10.1128/mBio.03552-20 | PubMed

34. **Daniel C A,** Dipendra G, Kenric A G, William H C, Cary A M (2014) Productive replication of human papillomavirus 31 requires DNA repair factor Nbs1. *J Virol* **88** https://doi.org/10.1128/jvi.00517-14 | PubMed

35. **Govind A S,** Clodagh C OS (2015) Viral and Cellular Genomes Activate Distinct DNA Damage Responses. *Cell* **162** https://doi.org/10.1016/j.cell.2015.07.058 | PubMed

36. **Shengli M,** Shijun Z, Jiayou X, Guoyu Y, Lei Z, Jiang W, et al. (2024) Alphaherpesvirus manipulates retinoic acid metabolism for optimal replication. *iScience* **27** https://doi.org/10.1016/j.isci.2024.110144 | PubMed

37. **James J C,** James M M, Douglas R H (2014) Histone deacetylase inhibitors improve the replication of oncolytic herpes simplex virus in breast cancer cells. *PLoS One* **9** https://doi.org/10.1371/journal.pone.0092919 | PubMed

38. **Yue D,** Yuqi L, Siyu C, Yuhang X, Hongjia C, Shuyuan Q, et al. (2024) Neuronal miR-9 promotes HSV-1 epigenetic silencing and latency by repressing Oct-1 and Onecut family genes. *Nat Commun* **15** https://doi.org/10.1038/s41467-024-46057-6 | PubMed

39. **Sheng-Li Ming M-HD,** Yang Jia-Ming, Guo Ya-Di, Pan Jia-Jia, Lu Wei-Fei, Wang Jiang, Zeng Lei, Chu Bei-Bei (2025) The targeted cytosolic degradation of class I histone deacetylases is essential for efficient alphaherpesvirus replication Mendeley Data. *Mendeley Data* https://doi.org/10.17632/yg5fgtvxzk.3

Peer reviews

Reviewer #1 (Public review):

Summary:

In this study, the authors propose that HSV-1 infection degrades the class I histone deacetylases HDAC1 and HDAC2. The MDM2 E3 ubiquitin ligase from the DNA damage response pathway is responsible for ubiquitinating these HDACs that are subsequently degraded via proteasomes. The authors hypothesize that HDAC degradation will cause hyperacetylation of viral chromatin and enable viral gene transcription.

Strengths:

The ubiquitination of HDAC1 & HDAC2 by Mdm2 and the mapping studies are clear.

Comments on revised version:

The authors enhanced their manuscript by more supportive data and providing clarification and the necessary corrections. However, a few more issues pertain:

(1) In Figure 4j at 2 h post-infection we typically see the input virus and not progeny virus production. The input seems to have about 1-log difference that is expected to impact the results.

(2) Figs 1A, 1E, 2H it seems unclear why ICP4 becomes detectable at 12 h post-infection in HeLa cells? How about other a-genes? How about other cells? ICP4 is typically detectable within 2-3 h post-infection.

(3) In responses 2-2, Fig 5K: An infection without transfection has not been included. This is important to understand kinetics of infection in transfected cells.

(4) Why HDAC1 with deleted NES does not accumulate or looks like it is degraded? Why then ICP4 does not accumulate?

https://doi.org/10.7554/eLife.110309.2.sa2

Reviewer #2 (Public review):

Summary:

The authors discovered that HDAC1/2 are degraded in HSV-1 and PRV infections. They attempted to establish a new mechanism by which HDAC1/2 are translocated to the cytoplasm to be degraded in HSV-1 infection, and the degradation causes changes in histone acetylation to affect the DDR pathway.

Strengths:

(1) Interesting findings of HDAC1/2 degradation during HSV-1 and PRV infection, and it may impact more than the virology field.

(2) Significant work to identify the ubiquitin site in HDAC1/2 and K63 linkage.

Comments on revised version:

The authors added experiments to address the previous comments. The added knockdown and overexpression experiments provided sufficient support for the proposed mechanism. The conclusions are now strengthened. However, a few essential controls are still missing.

(1) Figure 3K: How does the expression level of Flag-HDAC1 variants compare to the endogenous HDAC1 level? The stripe probed by Flag antibody should be reprobed by HDAC1 antibody. Also, how does the K74R mutant affect histone acetylation? Moreover, the numbers between the panels are hard to read and have not been explained.

(2) Figure 3M and 3L: DNA transfection per se frequently stimulates cell reactions that inhibit HSV-1 replication. Is the HSV-1 only sample transfected by empty vector or untransfected?

(3) Figure 4G-4J: What is the MDM2 knockdown efficiency?

(4) Figure 5F and line 400-401: "thereby preventing HDAC1 degradation-markedly impaired HSV-1 replication (Fig. 5F)." However, viral replication is not demonstrated in Figure 5F.

(5) Figure 5K: also need a control of empty vector. Furthermore, how does the HDAC1 □NES expression affect histone acetylation and DDR responses?

(6) Statements listed below are better moved to discussion after all data being presented. They are quite a stretch when looking at each figure by itself.

(i) Line 268-270: "Together, these findings indicate that HSV-1 selectively degrades class I HDACs, resulting in widespread histone hyperacetylation that fosters a chromatin state conducive to viral replication". ----may be okay for a statement.

(ii) Line 291-292: "providing initial evidence that HSV-1 infection promotes DDR activation through downregulation of HDAC1 expression"

(iii) Line 331-333: "Together, these results indicate that HSV-1 infection promotes K63-linked polyubiquitination of HDAC1/2 at conserved lysine residues, ultimately leading to their proteasomal degradation."

(iv) Line 334-336 is a repeated sentence.

https://doi.org/10.7554/eLife.110309.2.sa1

Author response:

The following is the authors' response to the original reviews.

> ***Reviewer #1 (Public review):***
>
> *Summary:*
>
> *In this study, the authors propose that HSV-1 infection degrades the class I histone deacetylases HDAC1 and HDAC2. The MDM2 E3 ubiquitin ligase from the DNA damage response pathway is responsible for ubiquitinating these HDACs that are subsequently degraded via proteasomes. The authors hypothesize that HDAC degradation will cause hyperacetylation of viral chromatin and enable viral gene transcription.*
>
> *Strengths:*
>
> *The ubiquitination of HDAC1 & HDAC2 by Mdm2 and the mapping studies are clear.*

> *Weaknesses:*
>
> *(1) Degradation of HDACs is observed late, at least 12-24 h post-infection (1 PFU/cell). Viral genes have been transcribed by that point, and the virus has replicated its genome. The kinetics do not match the proposed model.*

We sincerely thank the reviewers for their insightful and constructive feedback. The original low-MOI condition introduced asynchronous infection and obscured early events. We repeated the time course at high MOI (MOI = 5) in HeLa cells. Under these synchronized conditions, HDAC1/2 degradation is detectable by 2 hpi and pronounced by 4-6 hpi—preceding viral DNA replication (~3-4 h) and coinciding with true late gene expression (ICP4). These data (Author response image 1) show that HDAC1/2 depletion is an early, virus-directed event, not a late consequence.

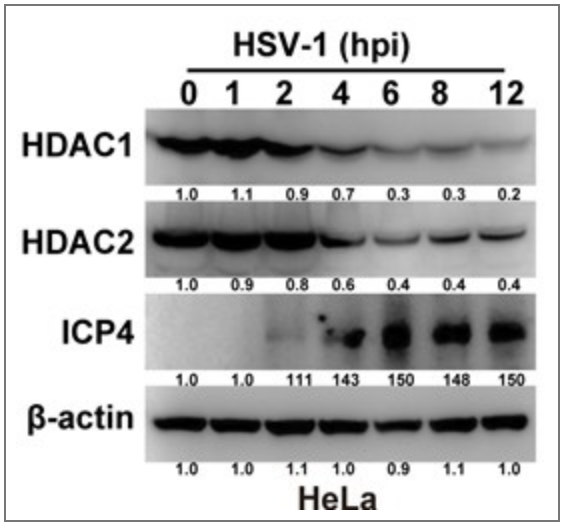

Author response image 1.

> *(2) The authors need to connect these findings with their story. As of now, these findings are correlative. For example, what is the impact of MDM2 depletion on viral gene expression and progeny virus production? Leptomycin B is not specific to the HDAC cytoplasmic translocation, and its effect on the infection could be due to its effect on ICP27.*

We generated stable MDM2 knockdown HeLa cells. MDM2 depletion reduced progeny virus titers at 24 hpi and suppressed ICP0, ICP8, and gB expression at both RNA and protein levels (Figure 4G-J). HDAC1/2 degradation was abolished (Figure 4B). Thus MDM2-dependent HDAC1/2 proteolysis is essential for the lytic transcriptional cascade.

To bypass LMB's broad CRM1 inhibition, we constructed an HDAC1 mutant lacking the nuclear export signal (HDAC1-ΔNES) that remains nuclear during infection. In HDAC1/2 double-knockdown cells, re-expression of HDAC1-ΔNES failed to rescue viral replication compared to wild-type HDAC1, and overexpression of HDAC1-ΔNES in control cells more strongly inhibited progeny yield (Figure 5K). This genetic approach confirms that HDAC1 nuclear export is specifically required for its proviral function, independent of ICP27.

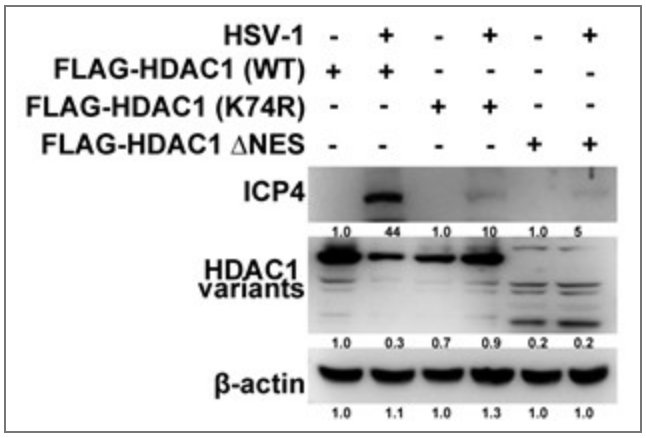

Author response image 2.

> *(3) The time point when the inhibitors were added to the cultures has not been stated in any experiment. If inhibitors were added with the virus, viral gene expression would be blocked.*

We sincerely thank the reviewers for identifying this critical oversight. Unless otherwise specified, All inhibitors were added at 1 hpi (post-adsorption) unless otherwise noted. Time-of-addition experiments for MG-132, LMB, and berzosertib are now included (Author response image 3, Figure 2K ,5A).

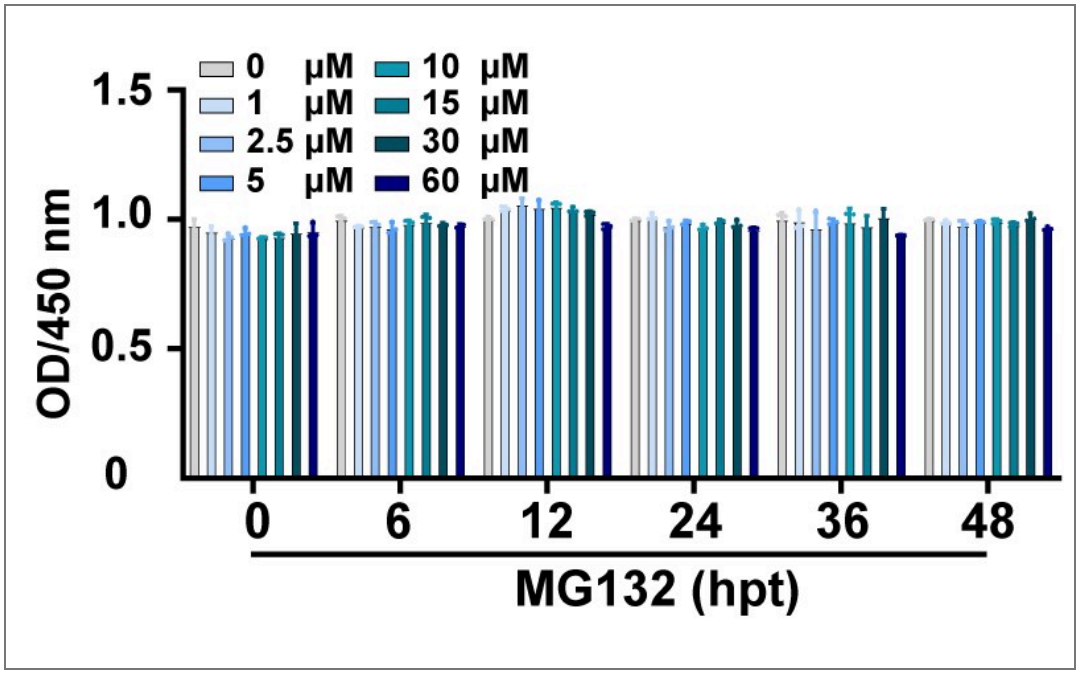

Author response image 3.

> *(4) The authors need to present late gene expression data in all the experiments where drugs have been used.*

In all drug-treated experimental conditions, we have performed comprehensive qRT-PCR analyses—quantifying mRNA levels of at least one immediate-early gene (ICP0), one early gene (ICP8), and one late gene (gB or gC)—to establish a temporally resolved viral gene expression profile across the entire replication cycle. This systematic assessment allows us to

rigorously determine whether the observed inhibitory effects are global or selectively restricted to specific kinetic classes of viral genes. Consistent with this design, both LMB and berzosertib significantly suppressed the mRNA expression of ICP0, ICP8, and gB in HSV-1–infected cells (Author response image 4), indicating that their antiviral activity likely stems from interference with an upstream regulatory node common to the transcriptional activation of immediate-early, early, and late viral genes.

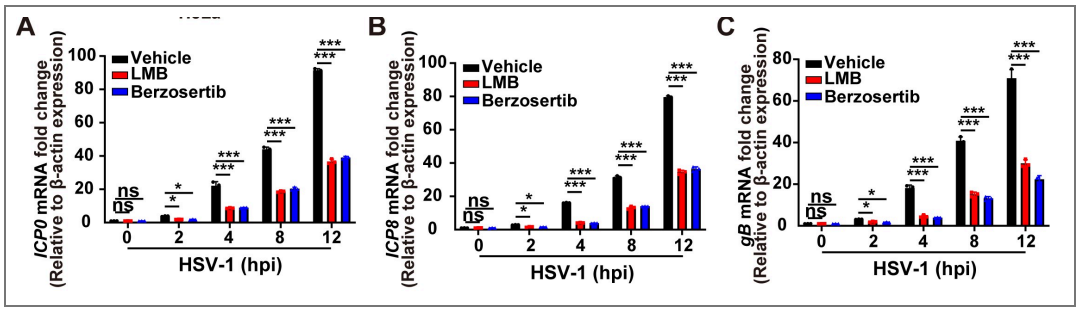

Author response image 4.

> *(5) Figure 1A, ICP4 is not detected up to 12 hours post-infection of HeLa cells with 1 PFU/cell. This cannot be true.*

This observation stems from technical artifacts in the original Western blot images—primarily insufficient signal intensity and suboptimal dynamic range. Therefore, we re-conducted the time-course experiment, systematically collecting samples at each time point and moderately increasing the sample loading volume while ensuring protein integrity. Optimized Western blot analysis confirmed robust ICP4 protein expression beginning at 12 hours post-infection, with progressive accumulation over time. Consequently, we have replaced all ICP4-related Western blot panels in Figure 1A, Figure 1E, and Figure 2H with newly acquired, rigorously exposure-calibrated images exhibiting high signal-to-noise ratios and unambiguous temporal resolution.

> *(6) Leptomycin B blocks nuclear/cytoplasmic shuttling of ICP27 that brings viral mRNAs to the cytoplasm to be translated. So, the effect of LMB is not specific to the HDACs.*

This is a critical point. As outlined in our response to Reviewer 2, we will address this issue through three complementary experimental approaches: (1) generation of an HDAC1 nuclear export signal (NES)–deficient mutant to genetically abrogate its nuclear export (Figure 5K); (2) rigorous nuclear-cytoplasmic fractionation coupled with immunoblotting to quantitatively assess HDAC1 subcellular distribution and site-specific ubiquitination. Importantly, our fractionation data confirm that HDAC1 ubiquitination is predominantly cytoplasmic (Figure 5F). Collectively, these experiments will rigorously distinguish direct HDAC1 modulation from indirect, LMB-mediated off-target effects—thereby ensuring the mechanistic specificity and interpretability of our conclusions.

> *(7) The key experiment is to use the degradation-resistant form of HDAC1 to evaluate its impact on viral gene transcription.*

Based on their comments, we systematically evaluated the effects of overexpression of wild-type (WT) HDAC1 and its ubiquitination site mutant K74R (anti-degradation form) on the transcription of HSV-1 viral genes and the yield of progeny viruses. Specifically, we measured the mRNA levels of representative immediate-early genes (ICP0), early genes (ICP8), and late genes (gB), and simultaneously determined the viral titer (Figure 3L). The results showed that compared with the empty vector control, overexpression of HDAC1 WT significantly inhibited the transcription of viral genes at all stages and reduced the yield of progeny viruses; while

overexpression of HDAC1 K74R exhibited a stronger inhibitory effect - its inhibition of viral gene transcription and viral replication was significantly higher than that of HDAC1 WT (Figure 3M). This result provides key functional validation for the core mechanism that "HSV-1 promotes its own replication by targeting the degradation of HDAC1/2 to relieve the epigenetic inhibition of its genome".

> *(8) In the experiment where Mdm2 was depleted, the authors need to demonstrate the effect on the infection. ICP4 expression is not enough. How about growth curves? After Mdm2 depletion, ICP4 expression increases, which may contradict the authors' findings. An analysis of alpha and gamma gene expression is important.*

We sincerely apologize to the reviewers for the error in Figure 4B, which arose from an oversight during experimental execution and data validation. We have rigorously repeated the experiment and confirmed that MDM2 knockdown robustly suppresses ICP4 protein expression—directly contradicting the erroneous upregulation depicted in the original figure. To fully characterize the functional consequences of MDM2 depletion on HSV-1 replication, we performed a multi-step viral growth assay and quantified mRNA levels of canonical viral genes by quantitative RT–PCR: consistent with the corrected ICP4 data, MDM2 knockdown significantly impaired progeny virus production and concurrently reduced transcript abundance of the immediate-early gene ICP0 and the early gene ICP8 (Figure 4G, 4H, 4I and 4J). We are profoundly grateful to the reviewers for identifying this critical discrepancy and for affording us the opportunity to provide a thorough correction and mechanistic clarification. In response, we have revised Figure 4B, updated all related text and figure legends, and conducted a comprehensive cross-check of all data, figures, and textual content across the manuscript.

> *(9) Why did the authors analyze a liver HSV-1 infection and not a more relevant skin infection?*

We sincerely apologize for the lack of sufficient detail in our prior response, which may have inadvertently increased the reviewers' evaluation burden. Prior to in vivo experimentation, we conducted a systematic tissue tropism profiling of HSV-1–infected mice, quantifying viral protein expression across multiple organs by Western blot (WB) (Author response image 5). This unbiased, multi-modal assessment demonstrated that the liver exhibited both the highest viral protein abundance and the greatest viral genomic load, coupled with the most pronounced and histologically reproducible pathology—including dense inflammatory infiltration, hepatocyte vacuolar degeneration, and sharply demarcated foci of necrosis. Importantly, HSV-1 infection induced a robust and coordinated downregulation of HDAC1 and HDAC2 protein levels specifically in the liver; this effect was neither as pronounced nor as consistent in other tissues examined. In contrast, although the skin serves as the natural portal of entry for HSV-1, it displayed consistently low and highly heterogeneous viral protein expression in this systemic model—rendering it unsuitable for rigorous virological or immunological quantification. Accordingly, grounded in these empirical findings and aligned with established practices in models of disseminated herpesvirus infection [1]—where the liver is routinely prioritized as the primary site of pathogenesis and immune interrogation—we designated the liver as the principal organ for in-depth analysis of viral replication dynamics and host innate and adaptive immune responses.

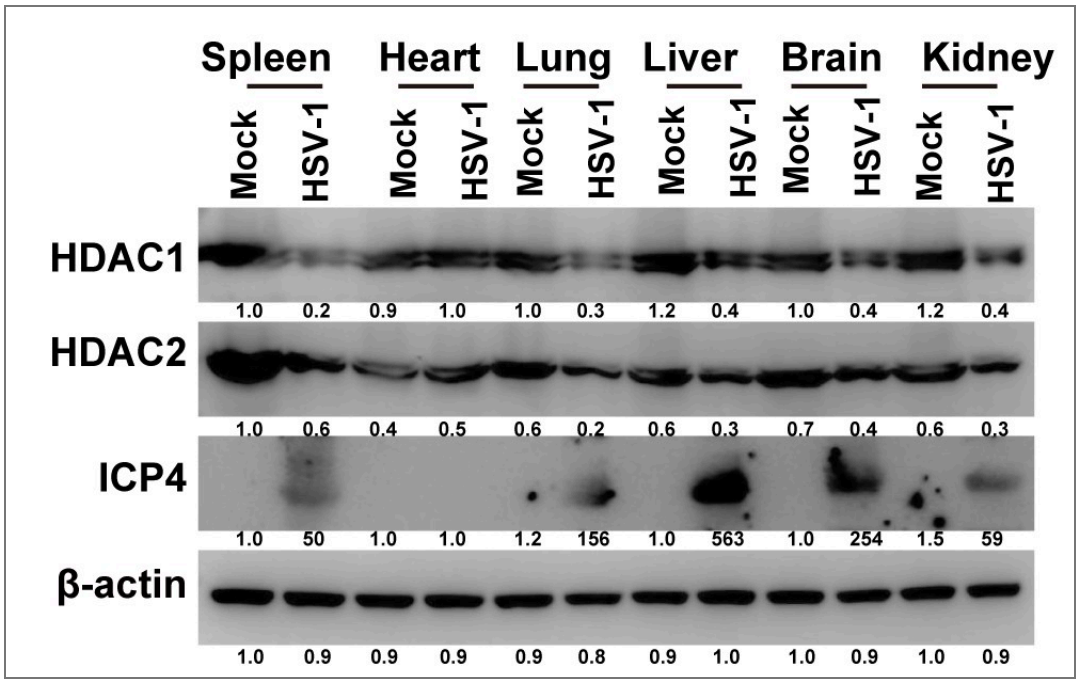

Author response image 5.

> ***Reviewer #1 (Recommendations for the authors):***
>
> *(1) It is an HDAC class and not cluss. All figures need correction.*

We sincerely apologize to the reviewers for this oversight and confirm that the error has been duly corrected in the revised manuscript.

> *(2) The authors need to quantify cells with H2AX in the nucleus in HSV-1 and PRV infections. Some blots from the analysis of the ATM signaling are not of great quality.*

As recommended, we performed quantitative immunofluorescence analysis to assess nuclear γ-H2AX foci formation in infected cells. Consistent with activation of the DNA damage response, γ-H2AX levels increased markedly in a time- and dose-dependent manner following HSV-1 or PRV infection. In addition, the immunoblot images for ATM signaling pathway components (Fig. 2H and 2I) have been replaced with higher-resolution.

> ***Reviewer #2 (Public review):***
>
> *Summary:*
>
> *The authors discovered that HDAC1/2 are degraded in HSV-1 and PRV infections. They attempted to establish a new mechanism by which HDAC1/2 are translocated to the cytoplasm to be degraded in HSV-1 infection, and the degradation causes changes in histone acetylation to affect the DDR pathway.*
>
> *Strength:*
>
> *(1) Interesting findings of HDAC1/2 degradation during HSV-1 and PRV infection, and it may impact more than the virology field.*
>
> *(2) Significant work to identify the ubiquitin site in HDAC1/2 and K63 linkage.*

We sincerely thank you for your positive assessment of this work and for your thoughtful, constructive feedback. Below, we provide point-by-point responses to each of your comments.

> *Weaknesses:*
>
> *(1) Insufficient evidence to support the mechanism described by the authors.*
>
> *(2) Expansion of the conclusion to alphaherpesvirus without studying the intended mechanism in PRV infection.*
>
> *Overall, there may be a correlation between HDAC1/2 level, ATM/ATR phosphorylation, and HDAC1 translocation during the HSV-1 infection. However, core evidence supporting the mechanism that a) HDAC1 export causes its degradation, b) degradation of HDAC1 causes histone acetylation changes and DRR activation has not been sufficiently demonstrated.*

In direct response to the central concern raised—that "the core experimental evidence supporting the proposed mechanistic model remains insufficient"—we have performed two complementary sets of rigorous validation experiments. Specifically, we addressed the two key mechanistic steps: (a) HDAC1 nuclear export is required for its ubiquitin–proteasome-dependent degradation; and (b) HDAC1 degradation drives histone hyperacetylation and consequent activation of the DNA damage response (DDR). Our new data robustly substantiate both causal links.

To establish causality between HDAC1 nuclear export and degradation, we employed a dual experimental approach: (i) generation of an HDAC1 nuclear export signal (NES) loss-of-function mutant (HDAC1-ΔNES), which specifically abrogates CRM1-mediated nuclear export without affecting protein stability or catalytic activity; and (ii) high-fidelity subcellular fractionation coupled with ubiquitin pull-down and quantitative immunoblotting, enabling precise quantification of HDAC1 distribution and site-specific ubiquitination across nuclear and cytoplasmic compartments. Consistent with our model, wild-type HDAC1 underwent pronounced cytoplasmic accumulation and polyubiquitination following HSV-1 infection, demonstrating that nuclear export is both necessary and sufficient for HDAC1 degradation.

To determine whether HDAC1 degradation functionally triggers downstream DDR activation, we generated stable HDAC1/2-knockdown HeLa cell lines using validated siRNA constructs. Loss of HDAC1/2 led to significant increases in H3 and H4 acetylation levels and robust induction of canonical DDR markers—including γ-H2AX foci formation, ATM phosphorylation, and ATR phosphorylation—phenocopying the effects observed during HSV-1 infection. These gain-of-function data confirm that HDAC1/2 depletion alone is sufficient to recapitulate the epigenetic and DDR phenotypes, thereby solidifying the mechanistic hierarchy: HDAC1 export → degradation → histone hyperacetylation → DDR activation.

> *(2) Expansion of the conclusion to alphaherpesvirus without studying the intended mechanism in PRV infection.*

Our prior work demonstrates that both porcine pseudorabies virus (PRV) and herpes simplex virus type 1 (HSV-1) elicit highly concordant phenotypic outcomes—including marked depletion of HDAC1/2 proteins, elevated acetylation of histones H3 (K9/K27/K56) and H4 (K8/K12), and robust activation of the DDR pathway—as evidenced by parallel assays across both viral systems. While mechanistic dissection was primarily pursued in the HSV-1 model—due to its well-established tractability for biochemical and genetic interrogation—PRV and HSV-1 are evolutionarily closely related α-herpesviruses sharing extensive conservation in genome organization, replication machinery, and key immune-modulatory effectors. Critically, all core phenotypes described herein were independently validated in PRV-infected cells (Figure 1A/B,1E/F,2A/B), thereby providing direct experimental support for generalizing the findings to the α-herpesvirus genus. Accordingly, the title's scope is both empirically justified and scientifically precise.

> ***Reviewer #2 (Recommendations for the authors):***
>
> *Major issues:*
>
> *(1) Line 26: "we uncover a novel mechanism by which alphaherpesviruses exploit the DDR pathway". A mechanism has not been clearly described. The authors showed DNA damage, phosphorylation of DDR components, and viral inhibition by berzosertib in Figure 2. The authors seem to imply that DDR activation is the result of HDAC1/2 degradation, but causation has not been established. Do nondegradable HDAC1/2 identified in Figure 3 affect the ATM/ATR pathways?*

We acknowledge that causal inference required further experimental substantiation. To address this, we first established stable HDAC1/2-knockdown HeLa cell lines using validated siRNA constructs. Loss of HDAC1/2 resulted in marked elevation of histone acetylation marks—including H3K9ac, H3K27ac, H4K8ac, and H4K12ac—and robust induction of canonical DDR markers, specifically γ-H2AX foci formation, ATM phosphorylation, and ATR phosphorylation (Figure 1H and 2J). These phenotypes closely recapitulated those induced by HSV-1 infection, supporting a gain-of-function relationship. Critically, these data demonstrate that HDAC1/2 depletion alone is sufficient to drive both histone hyperacetylation and DDR activation—thereby reinforcing the proposed mechanistic cascade: HDAC1 nuclear export → proteasomal degradation → histone hyperacetylation → DDR pathway engagement. Second, to directly test whether HDAC1 degradation is functionally required for DDR activation during infection, we compared the effects of ectopically expressing wild-type HDAC1 WT versus the degradation-resistant mutant HDAC1 K74R in HSV-1-infected cells. Consistent with our model, HDAC1 WT expression partially attenuated both DDR activation and viral replication, whereas HDAC1 K74R exerted significantly stronger suppression of both endpoints—indicating that blocking HDAC1 degradation potently restrains the virus-induced DDR response and impairs viral fitness (Figure 3K and 3M). Collectively, these complementary loss- and gain-of-function experiments provide convergent evidence for a causal role of HDAC1 degradation in orchestrating the DDR during α-herpesvirus infection.

> *(2) Line 30: "Strikingly, viral infection promoted nuclear export of HDAC1/2, followed by MDM2-mediated K63-linked polyubiquitination and proteasomal degradation in the cytoplasm". In Figure 5A, strong staining of HDAC1 is present in the nucleus, while a small fraction seems to be detected in the cytoplasm at 24 h infection with the vehicle treatment. Compared to vehicle treated mock infection, the HSV-1-infected cell has more HDAC1 staining, not less. The authors need to explain the contradictory results before reaching such a conclusion.*

With regard to the apparent discrepancy in HDAC1 subcellular localization depicted in Figure 5A, we have rigorously re-evaluated the immunofluorescence data. All samples were reimaged under strictly identical acquisition parameters—including exposure time, laser power, detector gain, and objective magnification—to eliminate technical variability. Quantitative analysis was performed on ≥100 randomly selected, non-overlapping cells per condition, with nuclear and cytoplasmic fluorescence intensities measured independently and normalized to yield the nuclear-to-cytoplasmic (N/C) ratio—a robust, internally controlled metric of HDAC1 redistribution. Complementing this, biochemical validation was carried out via subcellular fractionation followed by quantitative Western blotting, which confirmed a significant decrease in nuclear HDAC1 and concomitant accumulation in the cytoplasmic fraction at 24 h post-HSV-1 infection ($p < 0.001$ vs. vehicle-treated mock control). These findings fully corroborate our original model (Figure 5B and 5C). The elevated nuclear signal previously observed in Figure 5A arose from localized contrast enhancement applied during image processing—an artifact unrelated to biological abundance—and has now been replaced in the revised figure with raw, unprocessed images. Full details of imaging

protocols, quantification methods, and statistical analyses are provided in the updated figure legend and Methods section. We sincerely apologize for any confusion this may have caused.

> *(3) In Figure 5, LMB blocks the export of HDAC1 and has negative effects on HSV-1. LMB nonspecifically blocks the nuclear export of many factors. HSV-1 sensitivity to LMB has been investigated (PMID: 23740995). Is ICP27 involved in HDAC1 translocation? To clarify the causation, can the authors separate the nuclear and cytoplasmic fractions to detect the HDAC1/2 ubiquitination status? Does the K74R mutant prevent viral replication?*

This is a critical point. As outlined in our response to Reviewer 2, we will address this issue through three complementary experimental approaches: (1) generation of an HDAC1 nuclear export signal (NES)–deficient mutant to genetically abrogate its nuclear export (Author response image 2, Figure 5K); (2) rigorous nuclear-cytoplasmic fractionation coupled with immunoblotting to quantitatively assess HDAC1 subcellular distribution and site-specific ubiquitination. Importantly, our fractionation data confirm that HDAC1 ubiquitination is predominantly cytoplasmic (Figure 5F). Collectively, these experiments will rigorously distinguish direct HDAC1 modulation from indirect, LMB-mediated off-target effects—thereby ensuring the mechanistic specificity and interpretability of our conclusions.

Furthermore, to functionally validate the physiological relevance of HDAC1 degradation in HSV-1 replication, we systematically evaluated the impact of HDAC1 WT versus its ubiquitination-resistant K74R mutant on viral gene expression and progeny production. Using qRT–PCR, we quantified mRNA levels of representative immediate-early (ICP0), early (ICP8), and late (gB) viral genes (Figure 3L); parallel plaque assays measured infectious virus yield. Strikingly, HDAC1 K74R overexpression conferred significantly stronger suppression of viral transcription across all kinetic classes and reduced progeny titers to a greater extent than HDAC1 WT (Figure 3M). These gain-of-function data provide compelling functional evidence supporting the central model that “HSV-1 promotes its own replication by inducing proteasomal degradation of HDAC1/2 to alleviate epigenetic repression of its genome.”

> *(4) Figure 1E: The elevation of H4K8 and H4K12 seems to correlate to the disappearance of HDAC1/2 in the time points given. However, changes in H3K9, H3K27, and H3K56 occur between 0 and 6 hours, when HDAC1/2 levels show minimum changes. How are the experiments repeated? Can the bands be quantitated to better reflect a correlation?*

In direct response to the concerns raised, we have rigorously refined our experimental approach and expanded the dataset to strengthen mechanistic interpretation:First, to address the temporal heterogeneity inherent in low-multiplicity infections (MOI = l)—a condition that can obscure early virus–host regulatory dynamics—we performed synchronized time-course experiments in HeLa cells at a high multiplicity of infection (MOI = 5). Under these optimized conditions, HDAC1 and HDAC2 degradation is robustly detectable by 2 hours post-infection and reaches near-complete loss by 4–6 hours. Critically, this degradation kinetics precedes the onset of viral DNA replication (initiated at ~3–4 h) and coincides with the expression of true late viral proteins (e.g., ICP4), confirming that HDAC1/2 clearance is an active, early viral strategy—not a passive consequence of late-stage infection. These revised data position HDAC1/2 depletion as a causal, upstream regulator of the immediate-early-to-late transcriptional switch (Author response image 1).

Second, to enable rigorous quantitative correlation, we conducted densitometric analysis of all histone acetylation marks (H3K9ac, H3K27ac, H3K56ac, H4K8ac, H4K12ac) and HDAC1/2 protein levels across three independent biological replicates. Quantified values are presented as mean ± SD beneath each corresponding blot panel in Figure 1, and kinetic profiles are visualized using normalized line graphs. Strikingly, the rapid hyperacetylation of H3K9, H3K27, and H3K56 during 0–6 hours exhibits strong temporal concordance with HDAC1 depletion—supporting a direct functional link between HDAC1 loss and locus-specific histone hyperacetylation on the viral genome. see Author response image 1

> *Minor points:*
>
> *(1) Materials and Methods: How are mouse live tissues harvested, maintained, and infected?*

We sincerely apologize for the omission of methodological details in the original manuscript. In response to your insightful and constructive comments, we have comprehensively revised the "Methods" section (lines 92 to 102), adding detailed steps for in vitro processing of mouse tissues, including precise time points for sample collection after infection, and strictly defined in vitro infection conditions for herpes simplex virus type 1. These additions have significantly enhanced the reproducibility of the experiments, the rigor of the analysis, and the transparency of the techniques. We are deeply grateful for your thorough, meticulous, and highly valuable review comments, which have greatly improved the scientific quality of our work.

> *(2) Figure 1A: class, not cluss.*

We sincerely apologize to the reviewers for this oversight and confirm that the error has been duly corrected in the revised manuscript.

> *(3) Figure 2A, 2B: need a control to indicate which cells are infected.*

Regarding Figure 2A and 2B, we wish to clarify that the primary antibody against total H2AX was a mouse monoclonal antibody, whereas the anti-γ-H2AX antibody was a rabbit polyclonal antibody. Due to species incompatibility in multiplex immunofluorescence staining, simultaneous detection of γ-H2AX and viral proteins (e.g., HSV-1 ICP0 or PRV gB) using conventional two-color labeling was not feasible in those initial experiments. To rigorously address this concern, we performed additional, carefully controlled validation experiments: we conducted parallel immunofluorescence assays using the same rabbit anti-γ-H2AX antibody together with mouse monoclonal antibodies against HSV-1 ICP0 and PRV gB—employing appropriate species-matched secondary antibodies and stringent controls. As shown in the newly included data (Author response image 6), γ-H2AX foci intensity and nuclear signal intensity increased progressively in a time- and infection-dose-dependent manner, correlating robustly with viral antigen expression. These results provide direct, orthogonal support for our original conclusion that HSV-1 and PRV infection induce DNA damage signaling in host cells.

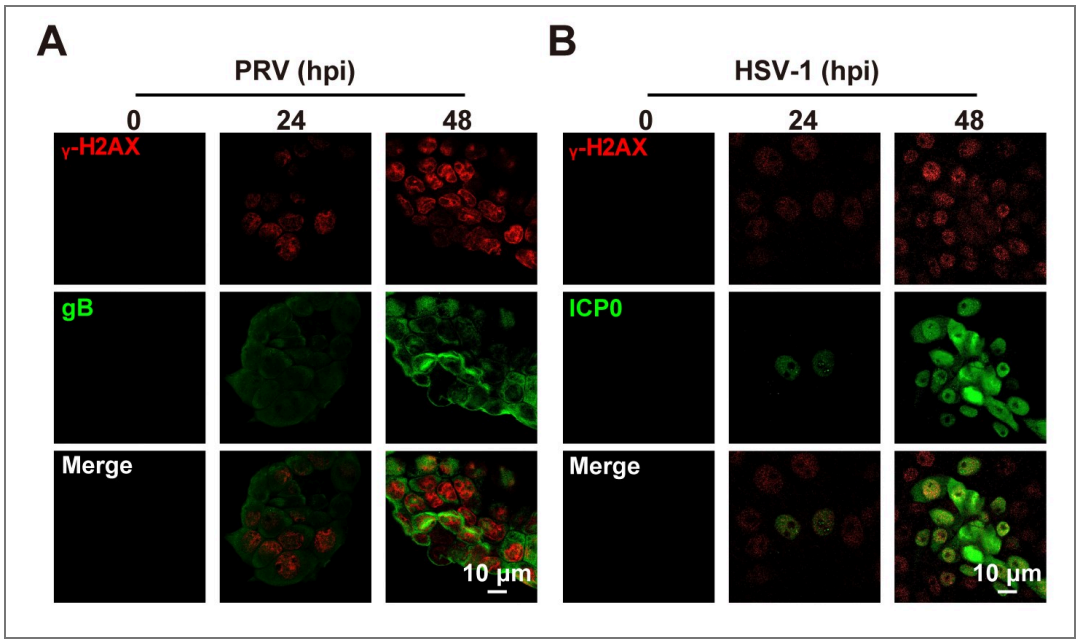

Author response image 6.

> *(4) Figure 4D, 4E; Why so small?*

We sincerely apologize for the confusion arising from the original figure layout. Figure 4D and 4E have now been revised to ensure accurate labeling, consistent scale bars, proper orientation, and full alignment with the corresponding descriptions in the text and legend.

> *(5) Does the level of endogenous MDM2 change under the experimental conditions of Figure 4?*

As demonstrated in Figure 4C—representing an endogenous co-immunoprecipitation assay—the protein level of endogenous MDM2 is markedly increased following viral infection. This result is consistently observed across biological replicates and is quantified in the accompanying immunoblot analysis (Figure 4C, lower panel), confirming robust upregulation of MDM2 expression under the experimental conditions.

> *(6) Line 359: "Our results are consistent across multiple cell types, including HeLa, 3D4/21, and murine liver". This statement is misleading. Only HeLa cells were used in Figures 3-5, which attempted to explain the mechanisms.*

We sincerely thank the reviewers for their careful reading and for identifying the inaccurate statements in the manuscript. All such statements have been revised, and the entire text has been systematically reviewed to ensure consistency, accuracy, and clarity across all sections.

> ***Reviewer #3 (Public review):***
>
> *The authors state that infection of cells by the alphaherpesviruses HSV-1 or PRV leads to a proteosome-dependent reduction in levels of HDAC1 and HDAC2 and that this leads to chromatin hyperacetylation, a DNA damage response, and greater replication of these viruses. Previously, other authors reported no change in levels of HDAC1 and HDAC2 after HSV-1 infection of human cells, but this paper is neither cited nor commented on in this new submission. The experiments are poorly designed. For instance, most of the time points analysed are way beyond the time needed for HSV-1 replication and are therefore not biologically relevant. The infections are done with a dose of virus that does not ensure that all cells are infected synchronously, but rather infection spreads from cell to cell with multiple rounds of replication. Some essential controls are missing. Additionally,*

> *this reviewer feels that the data presented do not support the conclusions drawn. Currently, links are not established between a reduction in HDAC1/ 2 and other phenomena such as hyperacetylation of histones, a DDR, and altered virus replication. The paper does not identify which HSV or PRV protein(s) induce reduction in HDACs, nor how the HDACs mediate antiviral activity; what are the HSV-1 or PRV protein targets? Lastly, the paper is not well prepared, and it does not adequately refer to prior literature.*

We sincerely thank the reviewers for their thoughtful, constructive, and highly valuable feedback. We deeply regret the shortcomings in our original submission—including incomplete literature coverage, insufficient mechanistic clarification, and gaps in experimental rigor—and fully acknowledge that these limitations affected the clarity and impact of our work. In response, we have comprehensively revised the manuscript: (i) expanded the literature review to incorporate key prior studies; (ii) added new experimental data—including time-resolved HDAC1/2 degradation assays, MDM2 knockdown/rescue experiments, and viral mutant analyses—to robustly substantiate the proposed mechanism; and (iii) rewritten the Results and Discussion sections to present a more precise, logically coherent, and evidence-based narrative. We are profoundly grateful for the reviewers' time, expertise, and guidance, which have significantly strengthened this study.

> ***Reviewer #3 (Recommendations for the authors):***
>
> *Major points*
>
> *(1) Failure to cite prior literature, incorrect in-text citations, and mistakes in the bibliography.*
>
> *(a) The authors do not refer to highly relevant prior literature. For instance, a proteomic study of HSV-1-infected human cells showed that HDAC1 and HDAC2 were stable during high MOI. (Soh et al., Cell Rep, 2020. 33, 108235). This paper must be cited, and the difference between the findings of these authors and the current submission must be addressed.*

We sincerely thank the reviewers for bringing to our attention the study by Soh et al. (Cell Reports, 2020, 33: 108235). After a thorough review, we found that the paper titled "Temporal Proteomic Analysis of Herpes Simplex Virus 1 Infection Reveals Cell-Surface Remodeling via pUL56-Mediated GOPC Degradation" does not report any changes in the protein abundance of HDAC1 or HDAC2 in its full text and supplementary data. We did not detect any significant differential expression or degradation of HDAC1/2 in the main figures, supplementary figures, quantitative proteomic data tables (Supplementary Tables S1–S3), or through a full-text keyword search of the original literature.

Furthermore, the other study that the reviewers might have in mind (Zhang et al., Cell Reports, 2019, 27: 1425–1438, DOI: 10.1016/j.celrep.2019.04.042) is about vaccinia virus (VACV) rather than HSV-1. It reports the degradation of HDAC5 and a transient downregulation of HDAC1 in the later stage of infection (see Figure 6E), but this downregulation did not reach statistical significance and was restored at subsequent time points. The study explicitly states that its findings do not apply to the HSV-1 infection system.

Therefore, the study by Soh et al. (2020) does not provide experimental evidence that HDAC1/2 remain stable under high MOI HSV-1 infection. We have added this clarification in the revised manuscript and will more rigorously distinguish the specificity of HDAC regulation in different herpesviruses and poxviruses in the discussion section to avoid cross-reference confusion. We are grateful to the reviewers for their insightful questions, which prompted us to conduct a systematic review of the relevant literature.

> *(b) In several instances, citations given in the text are not relevant to the statement made. For example, consider line 64 reference 12, line 67 reference 14, and line 76*

> *reference 22. The sentence preceding reference 12 is about the control of cellular gene expression by modulation of chromatin: the title of reference 12 is "Functional interaction between class II histone deacetylases and ICP0 of herpes simplex virus type 1". The sentence preceding reference 14 is about type IV HDACs (HDAC11), but the title of reference 14 is "Seneca Valley virus 3C protease cleaves HDAC4 to antagonize type I interferon signaling". HDAC4 is a type II HDAC. The sentence preceding reference 22 is HDAC1 facilitates STAT1 phosphorylation and enhances interferon-stimulated gene (ISG) activation, thereby restricting influenza A virus replication. The title of reference 22 is "Positive role of promyelocytic leukemia protein in type I interferon response and its regulation by human cytomegalovirus". I have not examined every citation, so there may be other examples of this. A thorough check of every statement and associated reference is needed.*

We sincerely apologize for the oversight in verifying and updating the accuracy of the cited references. All citations have now been thoroughly reviewed and corrected to ensure full alignment between each statement and its supporting source. We are deeply grateful to the reviewers for their careful scrutiny and constructive feedback, which greatly strengthened the rigor and reliability of our manuscript.

> *(c) The reference list is a mess. There are some references in which the given name of the authors is written, and the family name is abbreviated (incorrect), whereas in others the family name is written and the given name(s) are abbreviated (correct). I suspect this reflects the fact that in Mandarin, the family name is given first and the given names thereafter, whereas in English it is the other way round. But the inconsistency is careless, and modern reference management programs, such as EndNote, should eliminate these errors.*

We apologize for the errors in the original reference list and confirm that it has now been comprehensively revised: all entries have been uniformly reformatted in EndNote using the target journal's official citation style; author names have been standardized to surname followed by initials (e.g., "Smith J") in strict adherence to indexing and bibliographic standards; and all instances of underlined text, typographical inconsistencies, and grammatically incomplete sentences have been systematically identified and corrected.

> *Overall, the failure to cite relevant literature, the incorrect citations, and the incorrectly prepared bibliography are indicative of an unacceptable level of care in the preparation of this paper. As another example, consider lines 94-99. Why is the text underlined? And the last sentence is incomplete and does not make sense.*

The underlining in lines 94–99 was originally intended to highlight the experimental treatment protocols applied to the mice; however, we acknowledge that this formatting choice was inappropriate for a formal manuscript and could impair readability and professionalism. We have therefore removed all underlining in this section and revised the text to clearly and explicitly describe the mouse treatment procedures in complete, grammatically correct sentences.

> *(2) Virus infections have been done at 1 pfu/cell. This is a strange choice because the Poisson distribution shows that not all cells will be infected, and so after a first round of replication, the virus will spread sequentially from an infected cell to an uninfected cell. The fact that the level of HSV-1 protein gB is still increasing from 36-48 h pi (Fig. 1B) indicates that infection was very likely much less than 1 pfu/cell. Ditto for PRV (Figure 1). All infections must be redone at high moi (5-10 pfu/cell) so that the contribution of HDAC1 / 2 or the influence of specific pharmacological agents on the replication of virus in a single cycle can be determined. This is important because soluble factors released from infected cells can influence subsequent replication in the other cells. The release of these factors, or their influence on the uninfected cells, might be affected by the*

> *knockdown of HDACs or the addition of drugs tested. These concerns are largely eliminated by a high MOI (5-10 pfu/cell) so that all cells are infected synchronously.*

In direct response to the concerns raised, we have rigorously refined our experimental approach and expanded the dataset to strengthen mechanistic interpretation:First, to address the temporal heterogeneity inherent in low-multiplicity infections (MOI = 1)—a condition that can obscure early virus–host regulatory dynamics—we performed synchronized time-course experiments in HeLa cells at a high multiplicity of infection (MOI = 5). Under these optimized conditions, HDAC1 and HDAC2 degradation is robustly detectable by 2 hours post-infection and reaches near-complete loss by 4–6 hours (see Author response image 1). Critically, this degradation kinetics precedes the onset of viral DNA replication (initiated at ~3–4 h) and coincides with the expression of true late viral proteins (e.g., ICP4), confirming that HDAC1/2 clearance is an active, early viral strategy—not a passive consequence of late-stage infection. These revised data position HDAC1/2 depletion as a causal, upstream regulator of the immediate-early-to-late transcriptional switch.

> *(3) A one-step growth curve for HSV-1 in human cells is about 12 h. So most of the time points measured (e.g., 24, 3,6 and 48 h pi) are not biologically relevant.*

In response, we have repeated the HSV-1 one-step growth curve experiment under rigorously controlled high-MOI conditions (2 PFU/cell) and extended the kinetic sampling to include precise, biologically informative time points: 0, 1, 2, 4, 6, 8, 12, and 24 hours post-infection—thereby capturing the complete early-to-late replication cascade while excluding late-phase secondary spread (Figure 2L,4J and 5J).

Figure 2L,4J and 5J

> *(4) Figure 2I and Figure 5F show that the titer of HSV-1 obtained after infection of cultured cells reaches ~10e10 pfu/cell. This is extraordinarily high in comparison to a large body of HSV literature. Usually, the titer would be between 10e7 and 10e8 pfu/cell. The authors should explain what feature of their cell culture system enables production of infectious virus up to at least 100-fold greater than that of other investigators. The data shown in Figures 2I and 5F for "vehicle" look identical. If this is the same experiment, this should be stated, and it would be much better to show different data sets.*

First, we clarify that while the “vehicle” control data in Figure 2I and Figure 5F appear visually similar, they derive from independent biological replicates conducted on separate days under identical experimental conditions—not from the same assay (Author response image 7). Second, regarding the elevated viral titers (~10^10 PFU/cell) observed in our assays relative to typical literature values (10^7–10^8 PFU/cell), we confirm that the virus stock used is HSV-1 strain F (generously provided by Dr. Chun-Fu Zheng, University of Calgary, Canada), with a validated starting $TCID_{50}$ of ~10^7/mL. All infections were performed in standard growth medium (DMEM + 10% FBS), ruling out medium-related artifacts. Critically, our initial time-course design extended beyond the single-cycle window—leading to secondary spread and cumulative amplification. To address this, we rigorously re-optimized the assay: using a high MOI of 2 PFU/cell and sampling precisely at 0, 1, 2, 4, 6, 8, 12, and 24 hours post-infection, we consistently recapitulated the kinetics and magnitude of viral production(Figure 2L, 4J and 5J). We sincerely apologize for the oversight in our original experimental design and thank the reviewers for prompting this essential refinement.

Figure 2I

	Log10PFU/mL (HSV-1)								
	Vehicle			Berzosertib			Vehicle	Berzosertib
Times(h)	1#	2#	3#	1#	2#	3#	Mean	Mean
0	0	0	0	0	0	0	0	0
6	3.12	3	2.8	1.45	1.2	1.33	2.9733333	1.3266667
12	4.2	4	4.33	2.25	2.33	2.15	4.1766667	2.2433333
24	5.75	5.45	5.8	3.2	3.15	3	5.6666667	3.1166667
36	8.5	8.66	8.33	4	3.8	4.25	8.4966667	4.0166667
48	9.66	9.8	10	5.66	5.75	5.4	9.82	5.6033333

Figure 5F

	Log10PFU/mL (HSV-1)							
	Vehicle			LMB			Vehicle	LMB
Times(h)	1#	2#	3#	1#	2#	3#	Mean	Mean
0	0	0	0	0	0	0	0	0
6	2.15	2.66	2.4	1	1.15	1.2	2.403333	1.116667
12	4.9	4.5	4.66	2.5	2	2.2	4.686667	2.233333
24	6.5	6	6.2	3.8	4	3.66	6.233333	3.82
36	8.33	8.8	8.4	4.25	4.75	4.5	8.51	4.5
48	9.66	10	9.78	6.33	6	6.25	9.813333	6.193333

Author response image 7.

> *(5) Throughout the manuscript, there is little consideration given to the timing of the reduction in HDAC1/2 seen by immunoblotting, or the other changes such as hyperacetylation and DDR activation, in relation to the replication kinetics of the virus. These changes must occur early after infection to be able to influence virus replication. If they affect virus replication, what is the mechanism? At which stage during virus infection are they acting? What are the virus targets in HSV-1 or PRV-infected cells?*

First, we acknowledge the reviewers' important point that the temporal relationship between HDAC1/2 depletion (as detected by immunoblotting), concomitant histone hyperacetylation, DDR activation, and HSV-1 replication kinetics was not explicitly addressed in the original manuscript. As these host modifications must occur early post-infection to mechanistically influence viral replication, we have now performed time-resolved immunoblotting following high-MOI HSV-1 infection (MOI =5) and confirmed that HDAC1/2 protein levels begin to decline within 2–4 hours post-infection—well before the onset of robust viral DNA synthesis (typically detectable after 4–6 hpi) (see Author response image 1). Second, consistent with our prior work [2] and independent reports [3], the DDR can activate the cGAS–STING pathway, leading to upregulation of type I interferons and proinflammatory cytokines—established antiviral effectors. Notably, our previous study demonstrated that pharmacological or genetic inhibition of BRD4 induces DDR-dependent cGAS–STING activation and potently suppresses PRV replication [4]. In contrast, α-herpesviruses—including HSV-1 and PRV—actively subvert this antiviral axis by targeting HDAC1 and HDAC2 for MDM2-mediated K63-linked polyubiquitination and proteasomal degradation. This targeted depletion promotes histone hyperacetylation, chromatin decompaction, and a transcriptionally permissive environment that facilitates efficient viral gene expression and replication. Finally, regarding the reviewers' question about the specific viral determinant responsible for HDAC1/2 degradation, we fully agree that identifying the viral effector(s) is critical. Our ongoing studies are focused on systematically evaluating HSV-1 structural and non-structural proteins —including the E3 ubiquitin ligase activity of ICP0, the tegument protein VP16, and the viral kinase US3—to determine which factor(s) directly mediate MDM2 recruitment and HDAC1/2 ubiquitination. These experiments are underway and will be reported in future work.

> *(6) The manuscript does not demonstrate that a reduction in HDAC1 or HDAC2 is responsible for the changes in hyperacetylation. The virus induces many changes in the cell; others could also directly affect hyperacetylation. What about the activity of acetylases?*

To rigorously establish causality between HDAC1/2 depletion and histone hyperacetylation, we performed loss-of-function experiments using siRNA-mediated knockdown of HDAC1 and HDAC2 in uninfected cells. Immunoblotting analysis revealed a significant increase in acetylation levels of histone H3 (at lysines K9, K27, and K56) and histone H4 (at K8 and K12) upon HDAC1/2 depletion (Figure 1H)—mimicking the hyperacetylation pattern observed during HSV-1 infection. Importantly, no corresponding increase in histone acetyltransferase (HAT) activity was detected in HDAC1/2-knockdown cells, as assessed by in vitro HAT assays using nuclear extracts and confirmed by unchanged expression levels of major HATs (p300). These data demonstrate that HDAC1/2 loss alone is sufficient to drive global histone hyperacetylation, independent of alterations in acetyltransferase activity—and thus support a

direct mechanistic link between viral-induced HDAC1/2 degradation and the observed epigenetic changes.

> *(7) The study needs to make knockout cell lines, lacking HDAC1 or HDAC2 or both HDACs, and then test virus replication after high MOI in these cells. If a difference is seen, the missing HDAC should then be reintroduced into the knockout cell line under an inducible promoter, and the replication of the virus checked in these cells with or without induction of the HDAC. Furthermore, HDACs have many interacting partners; so to prove that it is the histone deacetylase activity of the HDAC that is causing a change in replication, cell lines that inducibly express each HDAC (derived from the corresponding knockout cell line) with the key residues needed for catalytic activity mutated, should be constructed, and the replication of the virus tested. As an example, HDAC4 is antiviral - but does this is independent of the histone deacetylase activity (Lu et al., PNAS 2019).*

To effectively address this comment, we successfully constructed HDAC1 single knockdown, HDAC2 single knockdown, and HDAC1/HDAC2 double gene co-knockdown cells using siRNA technology mediated by transfection reagents. We first confirmed that co-knockdown of HDAC1/2 robustly enhances histone H3/H4 acetylation and activates the DNA damage response (DDR), as evidenced by increased phosphorylation of H2AX (γH2AX), ATM, and ATR —consistent with the epigenetic and DDR phenotypes observed during HSV-1 infection (Figure 1H and 2J). To further clarify the functional significance of HDAC1 degradation and its subcellular localization during HSV-1 infection, we reconstituted HDAC1 in HDAC1 stably knockdown cells with: (i) wild-type HDAC1 (HDAC1-WT), (ii) a degradation-resistant mutant with ubiquitination site mutations (HDAC1-K74R), and (iii) a nuclear retention mutant lacking the nuclear export signal (HDAC1-ΔNES). The analysis of viral replication kinetics revealed that HDAC1 knockdown significantly increased the yield of progeny HSV-1; however, the reconstitution of HDAC1-WT completely reversed this phenotype, restoring the viral titer to the level of the unknockdown control. Crucially, both HDAC1-K74R and HDAC1-ΔNES exhibited stronger anti-HSV-1 replication activity than HDAC1-WT (Figure 5K), indicating that blocking the ubiquitin-dependent degradation of HDAC1 or forcing its retention in the nucleus can more effectively inhibit viral proliferation. In conclusion, these genetic data strongly support the model that HSV-1 actively promotes the nuclear export and K48-linked ubiquitination-mediated proteasomal degradation of HDAC1 to relieve its transcriptional repression on viral gene expression, thereby optimizing its replication environment (Figure 5K). These findings demonstrate that HSV-1 exploits HDAC1 degradation—and its subsequent cytoplasmic translocation—as a proviral strategy, and that preserving nuclear HDAC1 activity is intrinsically restrictive to viral replication. Regarding the reviewers' critical point on enzymatic specificity, we agree that definitive attribution to HDAC catalytic activity requires catalytically dead mutants (e.g., HDAC1-H141A/Y303F) expressed in isogenic HDAC1/2 knockout backgrounds under tightly regulated inducible systems. While such comprehensive genetic rescue experiments are technically demanding and beyond the scope of the current study, they represent a key focus of our ongoing work. Specifically, we are now systematically evaluating: (i) how HSV-1–mediated HDAC1 degradation mechanistically elevates histone acetylation at viral and host genomic loci; and (ii) the basis for functional divergence among HDAC family members—including differential expression, subcellular partitioning, interacting partners, and substrate selectivity—in regulating herpesviral replication. We deeply appreciate the reviewers' insightful guidance, which has significantly strengthened the mechanistic rigor and conceptual framework of this study.

> *(8) Figure 1C & D. The RT-qPCR data do not include analysis of a housekeeping gene against which the levels of mRNA for HDAC1 /2 can be compared. This is an essential missing control. The fact that the mRNA for gB is still increasing also confirms that the virus is still spreading, so the initial infection was most unlikely to have been at 1 pfu/cell.*

We confirm that all RT-qPCR data presented in Figure 1C and 1D were normalized to the endogenous control β-actin, and we have now explicitly stated this in both the Methods section and the corresponding figure legend. Regarding the observation that gB mRNA levels continue to rise over time, we agree that this reflects ongoing viral gene expression and progeny production—consistent with productive HSV-1 infection. However, this does not contradict our use of MOI = 1. In lytic herpesvirus infections, a single infectious particle initiates a cascade of gene expression, DNA replication, and assembly of new virions; therefore, increasing gB transcript levels across the time course are expected and reflect successful progression through the viral life cycle—not incomplete or suboptimal infection. Critically, Figures 1C and 1D were designed specifically to assess whether HSV-1 infection alters HDAC1/2 transcriptional regulation. The stable, MOI-independent expression of HDAC1/2 mRNA—despite progressive gB accumulation—demonstrates that the observed reduction in HDAC1/2 protein (shown in Figure 1A–B) is not due to transcriptional repression but rather results from post-translational mechanisms, such as virus-induced proteasomal degradation. This distinction strengthens our central conclusion: HSV-1 modulates host epigenetic machinery primarily via targeted protein destabilization, not transcriptional silencing.

> *(9) Figure 1G. The authors should explain how intranasal infection with HSV-1 leads to infection of the liver 5 days later. HSV-1 is neurotropic, not hepatotropic. Which types of liver cells are infected? Are they the same cells as the cells in which there are changes in acetylation? No evidence is presented to show that infection and acetylation changes are linked.*

We sincerely apologize for the lack of sufficient detail in our prior response, which may have inadvertently increased the reviewers' evaluation burden. Prior to in vivo experimentation, we conducted a systematic tissue tropism profiling of HSV-1–infected mice, quantifying viral protein expression across multiple organs by WB (Author response image 8). This unbiased, multi-modal assessment demonstrated that the liver exhibited both the highest viral protein abundance and the greatest viral genomic load, coupled with the most pronounced and histologically reproducible pathology—including dense inflammatory infiltration, hepatocyte vacuolar degeneration, and sharply demarcated foci of necrosis. Importantly, HSV-1 infection induced a robust and coordinated downregulation of HDAC1 and HDAC2 protein levels specifically in the liver; this effect was neither as pronounced nor as consistent in other tissues examined. In contrast, although the skin serves as the natural portal of entry for HSV-1, it displayed consistently low and highly heterogeneous viral protein expression in this systemic model—rendering it unsuitable for rigorous virological or immunological quantification. Accordingly, grounded in these empirical findings and aligned with established practices in models of disseminated herpesvirus infection [1]—where the liver is routinely prioritized as the primary site of pathogenesis and immune interrogation—we designated the liver as the principal organ for in-depth analysis of viral replication dynamics and host innate and adaptive immune responses.

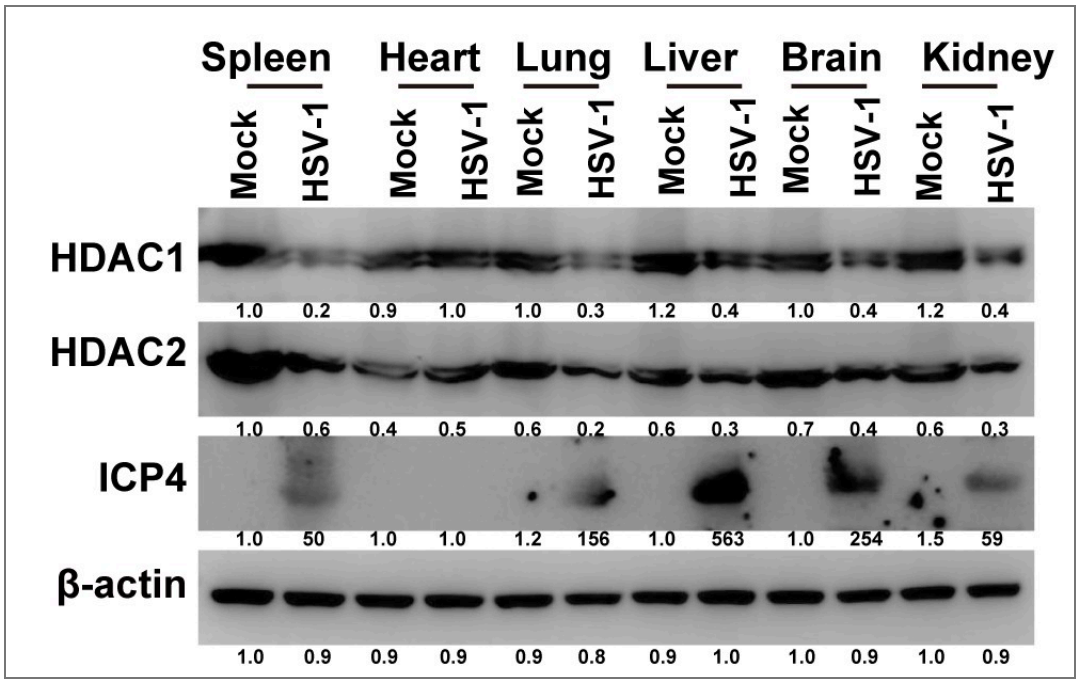

Author response image 8.

> *(10) Figure 1G. The 3 replicates show large variations from one sample to another at the same time point. Consider H3K9, H4K12, H3K56, for instance. A statistical analysis is needed to determine if these changes are significant, but this was not included.*

We sincerely appreciate the valuable suggestion from the reviewers. To address this, we performed quantitative densitometric analysis on all Western blot images presented in the manuscript. The band intensities were normalized to each sample as a reference, and the relative protein levels were further normalized to the value of the control (time zero or untreated) sample, which was set to 1.0. The resulting normalized quantification values are now displayed directly beneath each blot lane in Figures 1–5.

> *(11) Lines 233-5 and 254-8. These summary statements are not supported by the data presented. The authors have not established that these phenomena are linked.*

To directly address this point, we successfully constructed HDAC1/HDAC2 double gene co-knockdown cells using siRNA technology mediated by transfection reagents. We found that dual knockdown of HDAC1 and HDAC2 robustly enhanced histone H3/H4 acetylation and activated the DDR, as indicated by markedly increased phosphorylation of γH2AX, ATM, and ATR—phenotypes that closely recapitulate those observed during HSV-1infection (Figures 1H and 2J). These findings collectively establish a mechanistic link whereby HSV-1–mediated degradation of HDAC1/HDAC2 promotes histone H3/H4 acetylation and consequent DDR activation.

> *(12) Line 246. Comet assay. A description of what is being measured is needed here. To virologists, comet assays often look at plaque morphology.*

We acknowledge the omission in our original description and have added the requisite clarification at line 258.

> *(13) Figure 2I. Are these changes due to off-target effects of the drug? Cell viability assays are needed. And the authors should include an infection by a different virus that is not affected. Finally, the addition of the drug to cells lacking the target protein should be included - does this still influence virus replication?*

We sincerely thank the reviewers for their insightful suggestions. First, we assessed cell viability across all experimentally applied concentrations of Berzosertib using the CCK-8 assay and confirmed that none compromised cellular metabolic activity (Figure. 2K and 5A). Second, to control for virus-specific effects, we employed vesicular stomatitis virus (VSV) — a pathogen whose replication is independent of DDR activation — as a mechanistically distinct comparator. Consistent with this, Berzosertib treatment exerted no significant effect on VSV-GFP replication kinetics (Author response image 9), thereby excluding off-target contributions to the observed phenotypes.

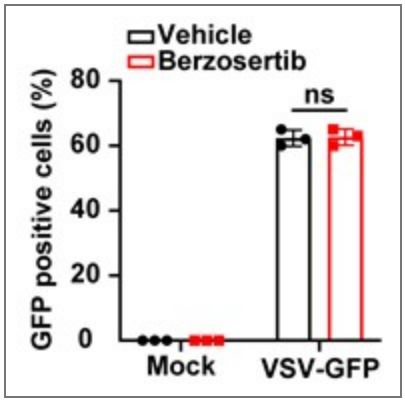

Author response image 9.

> *(14) Figure 3A. MG-132 is clearly antiviral - look at the big reduction in ICP4 - so the changes in HDAC1/2 levels +/- drug likely simply reflect different degrees of infection. The 24 and 36 h pi timepoints are too late to be biologically relevant.*

While it is well established that MG132 exhibits broad-spectrum antiviral activity—including inhibition of Classical swine fever virus (CSFV) [5], Hepatitis B virus (HBV) [6], and, to a lesser extent, Hepatitis C virus (HCV) and Hepatitis E virus (HEV) replication in vitro—its primary and most rigorously validated application in mechanistic virology and cell biology remains the pharmacological inhibition of the 26S proteasome. By specifically blocking the chymotrypsin-like activity of the proteasome core particle, MG132 induces rapid accumulation of polyubiquitinated substrates, thereby enabling researchers to: (i) determine whether a given protein is degraded via the ubiquitin–proteasome system (UPS); (ii) assess the kinetics of its turnover; and (iii) distinguish UPS-mediated degradation from alternative pathways such as autophagy–lysosomal degradation [7]. Critically, MG132 is not used here as an antiviral agent per se, but as a precise biochemical tool to interrogate the degradation mechanism of HDAC1/2 during HSV-1 infection.

> *(15) Figure 4. Since HDAC1 is degraded during infection, and the ligase responsible is claimed to be MDM2, HDAC1-MDM2 interaction would lead to the degradation of HDAC1/2, so less HDAC would be seen interacting with MDM2. To address this, the interaction analysis should be done in the presence of a proteosomal inhibitor such as MG132.*

We sincerely thank the reviewer for this insightful suggestion. To clarify: during HSV-1 infection, HDAC1 undergoes proteasomal degradation, a process that is strictly dependent on virus-induced ubiquitination—specifically, K48-linked polyubiquitination—which targets HDAC1 for recognition and binding by the E3 ubiquitin ligase MDM2. This ubiquitin-dependent interaction is a prerequisite for subsequent HDAC1 degradation via the 26S proteasome. While proteasome inhibition (e.g., with MG132) stabilizes HDAC1 protein levels and is routinely applied during co-immunoprecipitation (co-IP) sample preparation to

prevent artifactual degradation, it concurrently dampens the physiological ubiquitination signal required for efficient MDM2–HDAC1 engagement. Consequently, although HDAC1 abundance increases under MG132 treatment, the functional ubiquitin-mediated interaction between HDAC1 and MDM2 is attenuated—not enhanced—making MG132-treated conditions suboptimal for interrogating the physiologically relevant E3–substrate interaction. Critically, our co-IP experiments—performed in the absence of MG132 but with careful attention to rapid lysis, cold buffers, and protease inhibitors—still robustly detect HDAC1–MDM2 association despite ongoing degradation, thereby providing direct biochemical evidence that HDAC1 engages MDM2 in a ubiquitin-dependent manner during active infection.

> *(16) Figure 5. Lines 325-7. HSV replication is nuclear but requires export of mRNA and nascent capsids from the nucleus. So if any of these virus processes are influenced by leptomycin B, of course, the virus titer will be reduced. The link claimed is not proven。*

To better enhance the relevance of the article and further clarify the functional significance of HDAC1 degradation and its subcellular localization during HSV-1 infection, we reintroduced: (i) wild-type HDAC1 (HDAC1-WT), (ii) a degradation-resistant mutant with ubiquitination site mutations (HDAC1-K74R), and (iii) a nuclear retention mutant lacking the nuclear export signal (NES) (HDAC1-ΔNES) into HDAC1 stably knockdown cells. The analysis of viral replication kinetics revealed that HDAC1 knockdown significantly increased the yield of progeny viruses of HSV-1; however, the reintroduction of HDAC1-WT completely reversed this phenotype, restoring the viral titer to the level of the unknockdown control. Crucially, both HDAC1-K74R and HDAC1-ΔNES exhibited stronger anti-HSV-1 replication activity than HDAC1-WT (Figure 5K), indicating that blocking the ubiquitin-dependent degradation of HDAC1 or forcing its retention in the nucleus can more effectively inhibit viral proliferation. In summary, these genetic evidences strongly support the mechanism model that HSV-1 actively promotes the nuclear export and K48-linked ubiquitination-mediated proteasomal degradation of HDAC1 to relieve its transcriptional inhibition on viral gene expression, thereby optimizing its own replication environment.

References：

(1) B. Stefano et al., Two Fatal Cases of Acute Liver Failure Due to HSV-1 Infection in COVID-19 Patients Following Immunomodulatory Therapies. Clin Infect Dis 73, (2020).

(2) L. Guo-Li et al., Inhibition of PARP1 Dampens Pseudorabies Virus Infection through DNA Damage-Induced Antiviral Innate Immunity. J Virol 95, (2021).

(3) L. Tuo, C. Zhijian J, The cGAS-cGAMP-STING pathway connects DNA damage to inflammation, senescence, and cancer. J Exp Med 215, (2018).

(4) W. Jiang et al., BRD4 inhibition exerts anti-viral activity through DNA damage-dependent innate immune responses. PLoS Pathog 16, (2020).

(5) C. Yuming et al., MG132 Attenuates the Replication of Classical Swine Fever Virus in vitro. Front Microbiol 11, (2020).

(6) W. Yi, L. Xiao-Liang, Y. Yong-Sheng, T. Zheng-Hao, Z. Guo-Qing, Inhibition of hepatitis B virus production in vitro by proteasome inhibitor MG132. Hepatogastroenterology 60, (2013).

(7) H. Tianhua et al., Lipid peroxidation triggered by the degradation of xCT contributes to gasdermin D-mediated pyroptosis in COPD. Redox Biol 77, (2024).

https://doi.org/10.7554/eLife.110309.2.sa0